A&A 449, 723–736 (2006)
DOI: 10.1051/0004-6361:20053850
© ESO 2006

Astronomy & Astrophysics

Abundances of refractory elements in the atmospheres of stars with extrasolar planets⋆,⋆⋆,⋆⋆⋆

G. Gilli[1,2], G. Israelian[2], A. Ecuvillon[2], N. C. Santos[3,4], and M. Mayor[4]

[1] Dipartimento di Astronomia, Università degli Studi di Padova, Italy
[2] Instituto de Astrofísica de Canarias, 38200 La Laguna, Tenerife, Spain
e-mail: gil@iac.es
[3] Centro de Astronomia e Astrofísica da Universidade de Lisboa, Observatório Astronómico de Lisboa, Tapada da Ajuda, 1349-018 Lisboa, Portugal
[4] Observatoire de Genève, 51 ch. des Maillettes, 1290 Sauverny, Switzerland

Received 18 July 2005 / Accepted 6 December 2005

ABSTRACT

Aims. This work presents a uniform and homogeneous study of chemical abundances of refractory elements in 101 stars with and 93 without known planetary companions. We carry out an in-depth investigation of the abundances of Si, Ca, Sc, Ti, V, Cr, Mn, Co, Ni, Na, Mg and Al. The new comparison sample, spanning the metallicity range $-0.70 < [Fe/H] < 0.50$, fills the gap that previously existed, mainly at high metallicities, in the number of stars without known planets.
Methods. We used an enlarged set of data including new observations, especially for the field "single" comparison stars . The line list previously studied by other authors was improved: on average we analysed 90 spectral lines in every spectrum and carefully measured more than 16 600 equivalent widths (*EW*) to calculate the abundances.
Results. We investigate possible differences between the chemical abundances of the two groups of stars, both with and without planets. The results are globally comparable to those obtained by other authors, and in most cases the abundance trends of planet-host stars are very similar to those of the comparison sample.
Conclusions. This work represents a step towards the comprehension of recently discovered planetary systems. These results could also be useful for verifying galactic models at high metallicities and consequently improve our knowledge of stellar nucleosynthesis and galactic chemical evolution.

Key words. stars: abundances – stars: fundamental parameters – stars: low-mass, brown dwarfs – stars: planetary systems – Galaxy: solar neighbourhood – Galaxy: abundances

1. Introduction

Over the last ten years a large number of stars harbouring planets have been found. The first giant planet was discovered around 51 Peg by Mayor & Queloz (1995) and there are more than 150 planetary-mass companions presently known orbiting solar-type stars. The growing number of extrasolar planets[1] has activated intensive study of these objects and their parent stars, and nowadays extensive studies of the properties of the new planetary systems are conceivable. Several spectroscopic analyses of iron abundances (Gonzalez 1998; Gonzalez et al. 2001; Laws et al. 2003; Santos et al. 2001a,b, 2003, 2004a,b, 2005) have suggested that planet-host stars are more metal-rich than field dwarfs. These results show that the probability of finding a planet is a strongly increasing function of stellar metallicity, at least for [Fe/H] above solar value. Two interpretations, the *self-enrichment hypothesis* and the *primordial hypothesis*, have been proposed to explain a possible connection between the metallicity excess and the presence of planets. The former considers that the observed iron overabundances derives from the accretion of a large amount of rocky planetesimal material on to

⋆ Based on observations collected at the La Silla Observatory, ESO (Chile), with CORALIE spectrograph at the 1.2 m Euler Swiss telescope, and with the FEROS spectrograph at the 1.52 m ESO telescope, at the Paranal Observatory, ESO (Chile), using the UVES spectrograph at the VLT/UT2 Kueyen telescope, and with the UES and SARG spectrographs at the 4 m William Hershel Telescope (WHT) and the 3.5 m TNG, respectively, both at La Palma (Canary Islands).
⋆⋆ Tables 7–10 are only available in electronic form at http://www.edpsciences.org
⋆⋆⋆ Table 11 is only available in electronic form at the CDS via anonymous ftp to cdsarc.u-strasbg.fr (130.79.128.5) or via http://cdsweb.u-strasbg.fr/cgi-bin/qcat?J/A+A/449/723

[1] A complete updated table of known planets can be found at http://obswww.unige.ch/exoplanets

Article published by EDP Sciences and available at http://www.edpsciences.org/aa or http://dx.doi.org/10.1051/0004-6361:20053850

the star (Gonzalez 1997). The latter, the "primordial scenario", suggests that the iron excess in stars with planets just reflects the high metal content of the protoplanetary cloud from which stars and planets were formed (Santos et al. 2000, 2001a,b).

In this context, abundance trends of chemical species other than iron can give important clues in this debate, so that discriminating between these two possibilities will help in understanding how planetary systems form. Efforts have been made to analyse the chemical abundances of light elements (e.g. García López & Pérez de Taoro 1998; Gonzalez & Laws 2000; Ryan 2000; Deliyannis et al. 2000; Israelian et al. 2003a, 2004; Santos et al. 2002, 2004b), as well as other metals (e.g. Gonzalez & Laws 2000; Gonzalez et al. 2001; Smith et al. 2001; Takeda et al. 2001; Sadakane et al. 2002; Fisher & Valenti 2005). Most of these authors considered inhomogeneous comparison samples of field dwarfs from the literature that might be a source of systematic errors. The majority of these studies support the primordial hypothesis (Pinsonneault et al. 2001; Santos et al. 2001a,b, 2002; Sadakane et al. 2002), but evidence of pollution has been found for a few cases (Israelian et al. 2001, 2003a,b; Low & Gonzalez 2001).

Unbiased and homogeneous studies of Fe abundance in stars with and without planets have been performed by Santos et al. (2001a, 2003, 2004a, 2005). Similar studies have been recently carried out for elements other than iron. Refractory elements (some α and Fe-group elements) have been analysed by Bodaghee et al. (2003); all volatile elements (C, S, Zn, N, O) have been studied by Ecuvillon et al. (2004a,b, 2006) and Na, Al and Mg by Beirão et al. (2005). These studies all required a uniform high-metallicity comparison, given the lack of "single" field stars in the data for [Fe/H] > 0.1. We provide results using new and more precise atmospheric parameters from high quality spectra and also complete the high-metallicity comparison between the two samples.

In this paper we present a detailed, homogeneous and uniform study of Si, Ca, Ti, Sc, V, Cr, Mn, Co, Ni, Na, Mg and Al in a set of 101 planet-harbouring stars and a group of 93 solar-type stars with no known planets in the metallicity range $-0.70 <$ [Fe/H] < 0.45. We have made use of about 16 600 *EW*s measured to calculate the [*X*/H] ratio for each element and have plotted the results in the [*X*/H] vs. [Fe/H] and [*X*/Fe] vs. [Fe/H] planes.

2. Data

All the objects from the comparison sample belong to the CORALIE extrasolar-planets-finding programme[2]. The high resolution spectra are the same as those used by Santos et al. (2004a) to derive precise and uniform stellar parameters for 98 planet-host stars and 41 comparison sample "single" dwarfs in a volume-limited sample in the solar neigborhood (<20 pc). It should be pointed out that the star HD 219542 B was excluded from the planet-host list presented in Santos et al. (2004a) since the presence of a planet around this star has been rejected (Desidera et al. 2004). All our spectra were collected during several observing campaigns with the CORALIE spectrograph on the 1.2 m Euler Swiss Telescope, the FEROS spectrograph on the 2.2 m ESO/MPI Telescope (both at La Silla, Chile), the UVES spectrograph on the VLT/UT2 Kueyen Telescope (Paranal Observatory, ESO, Chile), the SARG spectrograph on the 3.5 m TNG and the UES spectrograph on the 4.2 m WHT (both at the Roque de los Muchachos Observatory, La Palma, Spain). The spectrograph and data characterisctics are listed in Table 2.

In order to extend the number of stars in a comparison sample, we added 48 FEROS spectra from Santos et al. (2005) and five new SARG spectra. We refer the reader to this paper for a description of the data. The S/N ratio of the spectra varies between 150 and 350. New high S/N spectra obtained in 2004 with VLT/UVES have been used as well (see Ecuvillon et al. 2004a,b, 2006)

3. Spectral analysis

Chemical abundances of the nine refractory elements studied here, as well as Na, Mg and Al, were derived performing a standard local thermodynamic equilibrium (LTE) analysis, strictly differential with respect to the Sun. Solar abundances for each element were taken from Anders & Grevesse (1989) using a solar model with $T_{\rm eff} = 5777$ K, $\log g = 4.44$ dex, $\xi_{\rm t} = 1.0$ km s^{-1}. We used a revised version (2002) of the MOOG code (Sneden 1973)[3] (with the *abfind* driver) and a grid of Kurucz (1993) ATLAS9 atmospheres. The atmospheric parameters, effective temperature ($T_{\rm eff}$), surface gravity ($\log g$), microturbolence ($\xi_{\rm t}$) and metallicity ([Fe/H]), and their corresponding uncertainties, were taken from Santos et al. (2004a, 2005). It should be stressed that these stellar parameters were derived in a uniform way, using high resolution spectra, the same line list and model atmospheres for all the stars. The spectral lines of the refractory elements analysed here were extracted from the study by Bodaghee et al. (2003), while the line lists of Na, Mg and Al were taken from Beirão et al. (2005). These lists were successively modified in order to minimize abundance errors. Since the V I line at 6531.42 Å, the Mn I line at 5388.50 Å and the Co I lines at 5312.86 Å and 6632.44 Å were difficult to measure in most of the spectra (too weak or blended), we eliminated them from the list. We also excluded the Mg line at 8923.57 Å because it was not measurable in the new Feros spectra analysed for Na, Mg and Al. We added more lines of V, Mn and Co from Gurtovenko & Kostik (1989). Before including these lines in our list, we first verified that each line was not too strong and checked for possible blending, using the Kurucz Solar Atlas (Kurucz et al. 1984). For these new lines we derived semi-empirical atomic oscillator strengths using their *EW*s measured in the solar atmosphere with ($T_{\rm eff}$, $\log g$, $\xi_{\rm t}$) = 5770 K, 4.44 dex and 1.0 km s^{-1}), and performed an inverted solar analysis. The number of lines increased from 5 to 9 for V, from 3 to 8 for Mn, and from 5 to 7 for Co.

Finally, we considered about 80 spectral lines for the analysis of refractory elements in each spectrum and about 14 lines

[2] http://unige.ch/~udry/planet/planet.html

[3] The MOOG2002 source code can be downloaded at http://verdi.as.utexas.edu/moog.html

Table 1. Atomic parameters of the spectral lines used for every element. Column 1: wavelength (in Å); Col. 2: excitation energy of the lower energy level in the transition (in eV); Col. 3: oscillator strengths based on an inverse solar analysis.

λ	χ_l	$\log gf$	λ	χ_l	$\log gf$
Si I; $\log\epsilon_\odot = 7.55$ $A = 14$			**Cr** I; $\log\epsilon_\odot = 5.67$ $A = 24$		
5665.56	4.92	−1.980	5304.18	3.46	−0.680
5690.43	4.93	−1.790	5312.86	3.45	−0.580
5701.10	4.93	−2.020	5318.77	3.44	−0.710
5772.14	5.08	−1.620	5480.51	3.50	−0.830
5793.09	4.93	−1.910	5574.39	4.45	−0.480
5948.55	5.08	−1.110	5783.07	3.32	−0.400
6125.02	5.61	−1.520	5783.87	3.32	−0.150
6142.49	5.62	−1.480	5787.92	3.32	−0.110
6145.02	5.61	−1.400	**Mn** I; $\log\epsilon_\odot = 5.39$ $A = 25$		
6155.15	5.62	−0.750	4265.92	2.94	−0.440
6721.86	5.86	−1.090	4470.13	2.94	−0.550
Ca I; $\log\epsilon_\odot = 6.36$ $A = 20$			4502.13	2.92	−0.490
5512.98	2.93	−0.440	5399.47	3.85	−0.0969
5581.97	2.52	−0.650	5413.68	3.85	−0.470
5590.12	2.52	−0.710	5432.54	0.00	−3.620
5867.56	2.93	−1.590	6440.93	3.77	−1.250
6161.29	2.52	−1.220	**Co** I; $\log\epsilon_\odot = 4.92$ $A = 27$		
6166.44	2.52	−1.120	5301.04	1.71	−1.930
6169.05	2.52	−0.730	5325.27	4.02	−0.120
6169.56	2.52	−0.440	5342.70	4.02	0.574
6449.82	2.52	−0.630	5483.36	1.71	−1.220
6455.60	2.52	−1.370	5647.23	2.28	−1.580
Sc II; $\log\epsilon_\odot = 3.10$ $A = 21$			6093.15	1.74	−2.340
5239.82	1.45	−0.760	6455.00	3.63	−0.280
5318.36	1.36	−1.700	**Ni** I; $\log\epsilon_\odot = 6.25$ $A = 28$		
5526.82	1.77	0.150	5578.72	1.68	−2.650
6245.62	1.51	−1.040	5587.86	1.93	−2.380
6300.69	1.51	−1.960	5682.20	4.10	−0.390
6320.84	1.50	−1.840	5694.99	4.09	−0.600
6604.60	1.36	−1.160	5805.22	4.17	−0.580
Ti I; $\log\epsilon_\odot = 4.99$ $A = 22$			5847.00	1.68	−3.410
5471.20	1.44	−1.550	6086.28	4.26	−0.440
5474.23	1.46	−1.360	6111.07	4.09	−0.800
5490.15	1.46	−0.980	6128.98	1.68	−3.370
5866.46	1.07	−0.840	6130.14	4.26	−0.950
6091.18	2.27	−0.460	**Na** I; $\log\epsilon_\odot = 6.33$ $A = 11$		
6126.22	1.07	−0.410	5688.22	2.104	−0.625
6258.11	1.44	−0.440	6154.23	2.102	−1.607
6261.11	1.43	−0.490	6160.75	2.104	−1.316
6303.76	1.44	−1.600	**Mg** I; $\log\epsilon_\odot = 7.58$ $A = 12$		
6312.24	1.46	−1.580	5711.09	4.346	−1.706
V I; $\log\epsilon_\odot = 4.00$ $A = 23$			6318.72	5.108	−1.996
5668.37	1.08	−1.00	6319.24	5.108	−2.179
5670.85	1.08	−0.460	8712.69	5.932	−1.204
5727.05	1.08	−0.000	8736.02	5.946	−0.224
5727.66	1.05	−0.890	**Al** I; $\log\epsilon_\odot = 6.47$ $A = 13$		
5737.07	1.06	−0.770	6696.03	3.143	−1.570
6090.21	1.08	−0.150	6698.67	3.143	−1.879
6216.35	0.28	−0.900	7835.31	4.022	−0.728
6285.16	0.28	−1.650	7836.13	4.022	−0.559
6452.31	1.19	−0.820	8772.87	4.022	−0.425
			8773.91	4.022	−0.212

for the study of Na, Mg and Al abundances (see Table 1) in 53 new FEROS and SARG spectra. We have measured about 16 600 equivalent widths in our spectra. For each spectral line *EW*s were measured by a Gaussian fit using the *splot* task within the "echelle" IRAF package[4]. Furthermore we employed a new program (IRAF scripts) written by N. C. Santos for automatic measure of the *EW*s of Na, Mg and Al lines. This program was previously used to measure the *EW*s of a list of Fe lines (Santos et al. 2005). Every measurement was taken carefully achieving the best agreement between lines profile and Gaussian fits. About 25% of the equivalent widths used to calculate abundances come from Bodaghee et al. (2003), whose stellar parameters have been updated by Santos et al. (2004a, 2005). Detailed observational data (e.g. line-by-line *EW*s for each element) are available as an electronic table (Table 11) at the Centre des Données Strasbourg (CDS).

3.1. Uncertainties

We have tested the dependence of our results on atmospheric parameters (Fig. 1) and refer the reader to the Figs. 1−2 by Beirão et al. (2005) for the plots of [X/Fe] (X = Na, Mg, Al) vs. $T_{\rm eff}$ and vs. log g. In Table 3 are listed the slopes of the [X/Fe] ratios for refractory elements as a function of $T_{\rm eff}$ for all stars in the distributions. We observe no characteristic trends for the majority of the elements studied. In the case of Ti, V and Co we note decreasing trends for the [X/Fe] ratio corresponding to $T_{\rm eff}$ values greater than 5500 K. This trend could be caused by NLTE effects which, however, contribute mostly in the case of the more metal-poor stars. We do not take NLTE effects into account because they are usually small in metal-rich stars for complex atoms such as iron (see Edvardsson et al. 1993; Thévenin & Idiart 1999). On the other hand, although NLTE effects have not been studied for a number of elements (e.g. V, Co, etc.), they are nonetheless not thought to alter the main conclusion of the present paper. Some unknown blended lines may also be responsible for these trends. In fact, the overestimation of *EW*s caused by the increasing blending effects becomes more severe at lower $T_{\rm eff}$.

The distribution of planet-hosts and non-planet-host stars as function of $T_{\rm eff}$ shows that the latter are on average cooler (see Fig. 2). To verify this, we selected randomly two subgroups of stars (planet and no-planet hosts) with the same $T_{\rm eff}$ distributions and obtained the [X/H] distribution for Ti, V and Co. We repeated this process for 200 randomly selected subgroups and calculated the average distribution for each element (Ti, V, Co). In Fig. 3 we observed the same behaviour as that found for all the stars analysed. In both cases the differences between average [X/H] for hosts and no-hosts are of the same order (see Table 6.

In contrast, systematic errors are difficult to locate but are largely reduced by good data quality and good instrumental resolution. Since we have analysed more than one line for each element (usually 7−8 lines) in a given star, the total dispersions around the average abundance are more significant

[4] IRAF is distributed by National Optical Astronomy Observatories, operated by the Association of Universities for Research in Astronomy, Inc., under contract with the National Science Fundation, USA.

Table 2. Spectrographs and data characteristics.

Spectrograph/Telescope	Observatory	Resolution ($\lambda/\Delta\lambda$)	Range (Å)
CORALIE/1.2-m Ewler Swiss	La Silla (Chile)	50 000	3800–6800
FEROS/1.52-m ESO	La Silla (Chile)	48 000	3600–9200
UVES/VLT 8-mKuyen UT2	Paranal (Chile)	110 000	4800–6800
SARG/3.5-m TNG	ORM (la Palma)	57 000	5100–10 100
UES/4-m WHT	ORM (la Palma)	55 000	4600–7800

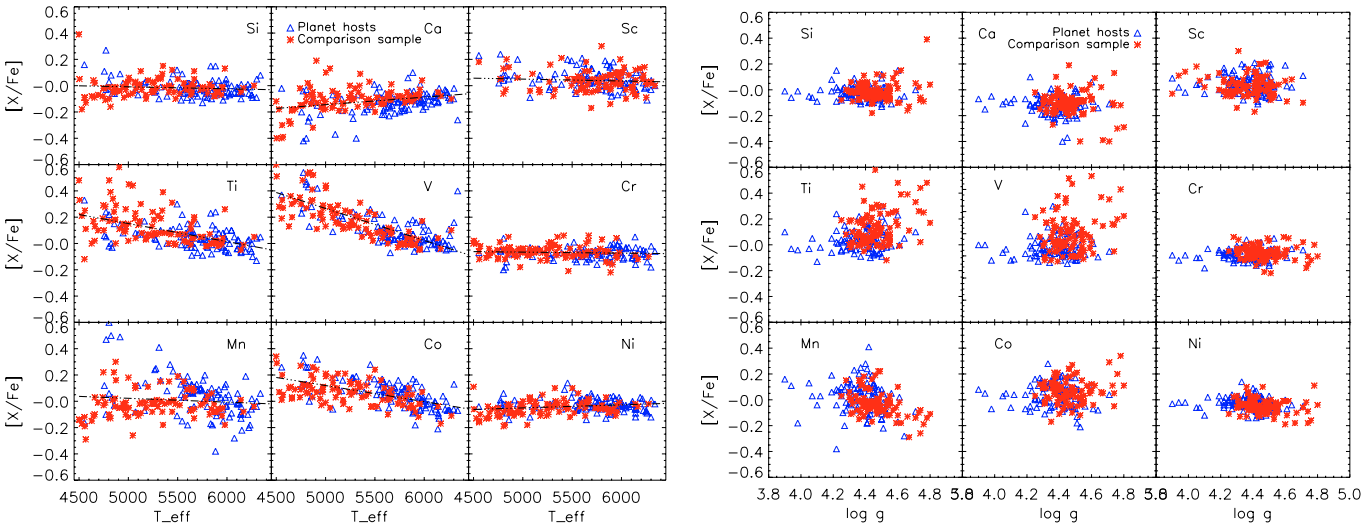

Fig. 1. [X/Fe] vs. $T_{\rm eff}$ and [X/Fe] vs. log g. Triangles and asterisks are planet host and comparison sample stars, respectively. Dotted lines represent the solar value. The slopes represent linear least-squares fits to both planet-hosts and comparison stars.

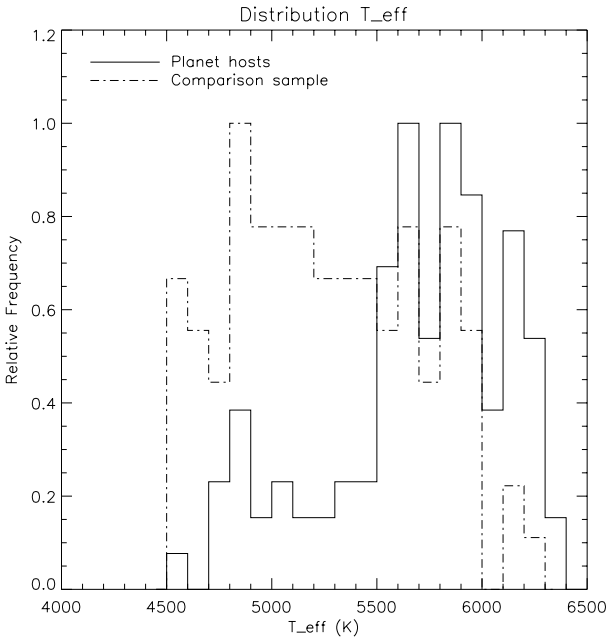

Fig. 2. Distributions of planet-host stars and non-planet-host stars as functions of $T_{\rm eff}$. The planet-host stars and the comparison sample are represented with solid and dotted lines, respectively.

compared to the continuum observed uncertainties, which are usually around 0.05 dex.

When analysing many lines to calculate abundances, uncertainties in the atmospheric parameters should be the primary source of abundance errors. These are of the order of 50 K in $T_{\rm eff}$, 0.12 dex in log g, 0.08 km s^{-1} in $\xi_{\rm t}$ and 0.05 dex in [Fe/H] (see Santos et al. 2004b, 2005). The abundance sensitivity to changes in atmospheric parameters were estimated as follows. First we selected a set of 12 stars from our list: for each atmospheric parameter we chose three stars with similar values for all the parameters except for the one considered, which must vary within the sample. We then generated new atmospheric models, changing only the "varying" parameter and calculating the corresponding abundances. The difference between these values and those obtained without varying the parameter, give us the abundance sensitivity to changes in the parameters. Tables 4 and 5 show these results after varying the effective temperature by $\Delta T_{\rm eff}$ = ±100 , surface gravity by Δ log g = ±0.30 dex, metallicity by Δ[Fe/H] = ±0.30 dex and microturbulence by $\Delta\xi_{\rm t}$ = ±0.50 km s^{-1}. We note that ions such as Sc II are generally more sensitive to changes in surface gravity, while neutral atoms are influenced mostly by uncertainties in the effective temperature. At a glance, we observe from Table 4 that the V and Ti abundances can vary with temperature changes of Δ[X/H] ∼ ±0.12 dex, while we associate Δ[Sc/H] ∼ ±0.11 dex with changes in surface gravity. With respect to Table 5 we note that Na abundances are more sensitive to variations in atmospheric parameters (e.g. $T_{\rm eff}$ and log g)

Table 3. Slopes of [X/Fe] ratios as functions of effective temperatures per 1000 K (in dex) for both samples (planet hosts and non-hosts).

Species	Slopes ± rms	Species	Slopes ± rms
Si	−0.015 ± 0.010	Cr	−0.007 ± 0.007
Ca	0.057 ± 0.013	Mn	−0.029 ± 0.020
Sc	−0.014 ± 0.011	Co	−0.122 ± 0.012
Ti	−0.137 ± 0.015	Ni	0.023 ± 0.008
V	−0.242 ± 0.015		

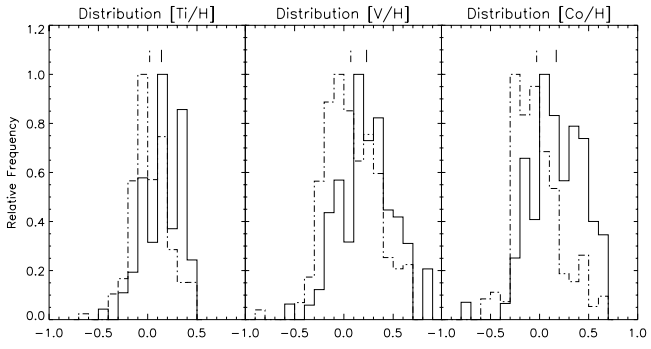

Fig. 3. [X/H] distributions for Ti, V and Co for the two subsamples of planet host (solid line) and comparison sample (dotted lines) stars with the *same* $T_{\rm eff}$ distributions.

than Mg and Al. Finally, we evaluated the errors in the abundances of all the elements, adding quadratically the standard deviation of the mean abundance obtained from all the measured lines and the uncertainties dued to the abundance sensitivities to changes in the atmospheric parameters. For each star these "total" errors are of the order of 0.10 dex.

4. Results

Bodaghee et al. (2003) recently carried out a spectroscopic analysis of the same refractory elements as those presented in our work while Beirão et al. (2005) did the same for Na, Mg and Al. These authors did not find any significant differences between planet host and comparison-sample stars, a result in perfect agreement with our findings. Because of the lack of comparison sample stars with [Fe/H] $>$ 0.1 dex in previous studies, the abundance distribution of stars with giant planets looked like a high metallicity extension of the curves traced by field dwarfs without planets. New spectra of metal-rich stars with no planets have been gathered, and consequently a complete comparison is also possible in the high metallicity domain. It is still conceivable that certain specific trends found for the metal-rich tail of Galactic chemical evolution are due to the presence of planets (see plots for Co, V, Na, Mg, Al in Figs. 7, 10). However, we should stress that even the new comparison sample contains about 20% of stars at [Fe/H] $>$ 0.1. All the results, together with their total errors (see Sect. 3.1), are listed in the Tables 7−10. Furthermore, we have compared the abundances calculated with *EW* values measured with different instruments. As shown in Fig. 4, we did not detect any significant discrepancies among the abundance values for the nine refractory elements.

The histograms provide the distributions of [X/H] with X = Si, Ca, Sc, Ti, V, Cr, Mn, Co and Ni (Fig. 6), and with X = Na, Mg, Al (Fig. 9) for the two samples of stars, with and without planets. These results are similar to those presented for [Fe/H] by Santos et al. (2004a, 2005) and clearly confirm that the observed metallicity excess is, as expected when extended to elements other than iron. We observe similar features to those noted in the [X/H] distribution for refractory elements (Bodaghee et al. 2003) and for iron (Santos et al. 2001a, 2004a; Reid 2002). For example, these histograms of planet-host stars are usually not symmetrical. This interesting feature is particularly evident for Ca, Sc, Co, Ni, Na and Al, for which the distribution seems to be an increasing function of [X/H] up to a certain value, after which it falls abruptly. This cut-off corresponds to [X/H] $\sim$ 0.5 for Si, Ti, Ni, Na, [X/H] $\sim$ 0.7 for V, Cr, Mn and Co and [X/H] $\sim$ 0.6 for Mg and Al. Only in the case of Ca does the distribution fall to [X/H] $\sim$ 0.3. For some elements (e.g. Ti, V, Cr, Mg) the distributions appear to be slightly bimodal. This is probably related to a lack of stars with [X/H] $\sim$ 0.3 in the planet-host sample and [X/H] $\sim$ −0.2 in the comparison group for these elements. The average values $\langle$[X/H]$\rangle$, the rms dispersions for the two distribution, and the difference between the average [X/H] for stars with and without planets are listed in Table 6. We note that this difference varies from 0.13 dex for V to 0.29 dex for Mn and Na. The difference between the average abundance values of the two groups (see Table 6) is only an estimate and is not very significant, given the usually high dispersion around the mean values.

In Fig. 5 are shown [X/H] vs. [Fe/H] plots for refractory elements. The [X/H] ratio is a linear function of [Fe/H] and the small amount of scatter give a certain plausibility to our results. We refer the reader to the Fig. 5 by Beirão et al. (2005) for the plots of [X/H] vs. [Fe/H] (X = Na, Mg and Al). These plots are not presented here because adding 52 new comparison sample stars did not change the results for these elements. However, [X/Fe] vs. [Fe/H] plots for Na, Mg and Al are shown in Fig. 10.

5. Galactic chemical evolution trends

With the exception of the lightest elements (e.g. H and He), the history of the Galaxy's chemical composition is dominated by nucleosynthesis occurring in many generations of stars (McWilliam 1997). The low-mass stars are like "fossils" because their lifetimes are sometimes comparable to the age of the Galaxy. It might actually be supposed that, at least for F–G dwarfs, the external envelope of the stars have preserved much of their original chemical composition, since it has not been convectively mixed with internal matter. The relation [X/Fe] vs. [Fe/H] is traditionally used in observational studies of the chemical evolution of the Galaxy since iron is a good chronological indicator of nucleosynthesis (controversial). Furthermore, iron lines are numerous and easy to measure in the spectra of dwarfs.

In Fig. 10 we present [X/Fe] vs. [Fe/H] plots for Na, Mg and Al taken from the work by Beirão et al. (2005) with the addition of abundances from a new comparison sample. We

Table 4. Sensitivity of the abundances of Si, Ca, Sc, Ti, V, Cr, Mn, Co and Ni to changes of 100 K in $T_{\rm eff}$, 0.30 dex in $\log g$ and [Fe/H], 0.50 km s^{-1} in $\xi_{\rm t}$.

Star ($T_{\rm eff}$; [Fe/H]; $\log g$; $\xi_{\rm t}$)	Si	Ca	Sc	Ti	V	Cr	Mn	Co	Ni
Temperature variation $\Delta T_{\rm eff}$ ± 100 K									
HD 50281A	∓0.06	±0.12	∓0.01	±0.14	±0.15	±0.06	±0.05	±0.01	∓0.01
(4685; −0.04; 4.32; 0.64)									
HD 43162	±0.01	±0.08	∓0.01	±0.10	±0.11	±0.06	±0.06	±0.06	±0.05
(5633; −0.01; 4.48; 1.24)									
HD 10647	±0.03	±0.07	∓0.01	±0.09	±0.10	±0.05	±0.06	±0.07	±0.06
(6143; −0.03; 4.48; 1.40)									
Surface gravity variation $\Delta \log g$ ± 0.30 dex									
HD 10697	±0.00	∓0.06	±0.11	∓0.01	∓0.01	∓0.01	∓0.02	±0.01	±0.00
(5641; 0.14; 4.05; 1.13)									
HD 168443	±0.01	∓0.07	±0.12	∓0.01	∓0.00	∓0.02	∓0.02	±0.01	±0.00
(5617; 0.06; 4.22; 1.21)									
HD 28185	±0.00	∓0.09	±0.11	∓0.02	∓0.02	∓0.03	∓0.04	±0.02	±0.01
(5656; 0.22; 4.45; 1.01)									
Metallicity variation Δ [Fe/H] ± 0.30 dex									
HD 6434	±0.01	±0.00	±0.06	∓0.01	∓0.01	±0.00	±0.00	±0.00	±0.00
(5835; −0.52; 4.60; 1.53)									
HD 147513	±0.00	±0.02	±0.08	∓0.01	∓0.01	±0.00	±0.00	±0.01	±0.01
(5894; 0.08; 4.43; 1.26)									
HD 4203	±0.00	±0.03	±0.10	∓0.00	∓0.01	±0.01	±0.02	±0.03	±0.04
(5636; 0.40; 4.23; 1.12									
Microturbulence variation $\Delta\xi_{\rm t}$ ± 0.50 km s^{-1}									
HD 69830	∓0.02	∓0.07	±0.01	±0.00	∓0.07	∓0.04	∓0.08	∓0.06	∓0.06
(5410; −0.03; 4.38; 0.89)									
HD 43162	∓0.02	∓0.08	∓0.06	∓0.05	∓0.04	∓0.04	∓0.08	∓0.05	∓0.05
(5633; −0.01; 4.48; 1.24)									
HD 84117	∓0.02	∓0.08	∓0.06	∓0.05	∓0.04	∓0.05	∓0.05	∓0.02	∓0.04
(6167; −0.03; 4.35; 1.42)									

also did calculations relative to the iron abundances ([X/Fe]) of α elements (e.g. Si, Ca, Ti) and of iron-peak elements (e.g. Cr, Mn, Co, Ni). The former are believed to be mostly produced in the aftermath of explosions of type II supernovae (SNe II), although, following some models, these elements might also be produced during a type Ia supernova (SN Ia) event (Thielmann et al. 2002). Meanwhile, most of the latter would have been synthesized by SNe Ia explosions. Magnesium is supposed to be produced by SNe II, thus comparing Mg abundances with those found for other α elements could provide us with evidence concerning the origin of these elements. Sodium and aluminium are thought to be mostly a product of Ne and C burning in massive stars. It is not clear how Sc is formed, because in the periodic table it is intermediate between α and iron-peak elements. The origin of manganese is also debated. However, Sc and Mn abundances in long-lived F and G stars are of great interest since they could also introduce special constraints on nucleosynthesis theory (Nissen et al. 2000). Even though the main aim of this study was to compare the abundances of refractory elements in stars with and without planets, our results also give us a chance to increase our present knowledge of the chemical evolution of the Galaxy at [Fe/H] > 0. In Figs. 7 and 10 we present the [X/Fe] vs. [Fe/H] plots for all the elements.

6. Comparison with the literature

There are already several studies concerning the chemical abundances of elements other than iron in F, G, K main sequence stars in the solar neighborhood (see Edvardson et al. 1993; Feltzing & Gustafsson 1998; Chen et al. 2000; Nissen et al. 2000; Fulbright et al. 2002; Reddy et al. 2003; Bensby et al. 2003; Allende Prieto et al. 2004). In addition, various studies on chemical abundances in planet-host stars have gradually emerged (Gonzalez et al. 2000; Santos et al. 2000; Takeda et al. 2001; Sadakane et al. 2002; Bodaghee et al. 2003; Ecuvillon et al. 2004a,b; Beirão et al. 2005;

Table 5. The same as Table 4 but for Na, Mg and Al.

Star ($T_{\rm eff}$; [Fe/H]; log g; $\xi_{\rm t}$)	Na	Mg	Al
Temperature variation $\Delta T_{\rm eff}$ ± 100 K			
HD 50281A	±0.09	±0.00	±0.07
(4685; −0.04; 4.32; 0.64)			
HD 43162	± 0.05	±0.05	±0.05
(5633; −0.01; 4.48; 1.24)			
HD 10647	±0.05	±0.05	±0.05
(6143; −0.03; 4.48; 1.40)			
Surface gravity variation $\Delta \log g$ ± 0.30 dex			
HD 10697	∓0.12	∓0.05	∓0.02
(5641; 0.14; 4.05; 1.13)			
HD168443	∓0.11	∓0.05	∓0.03
(5617; 0.06; 4.22; 1.21)			
HD 28185	∓0.05	∓0.03	∓0.03
(5656; 0.22; 4.45; 1.01)			
Metallicity variation Δ [Fe/H] ± 0.30 dex			
HD 6434	∓0.01	∓0.04	∓0.01
(5835; −0.52; 4.60; 1.53)			
HD 147513	±0.02	∓0.04	±0.00
(5894; 0.08; 4.43; 1.26)			
HD 4203	±0.02	±0.06	±0.00
(5636; 0.40; 4.23; 1.12			
Microturbolence variation $\Delta\xi_{\rm t}$ ± 0.50 km s^{-1}			
HD 69830	∓0.02	∓0.04	∓0.02
(5410; −0.03; 4.38; 0.89)			
HD 43162	∓0.02	∓0.04	∓0.02
(5633; −0.01; 4.48; 1.24)			
HD 84117	± 0.02	±0.04	∓0.03
(6167; −0.03; 4.35; 1.42)			

Fischer & Valenti 2005). We note that our abundance trends generally agree with those published in the literature and this lends a certain reliability to our results. In the following subsections, we describe [X/Fe] vs. [Fe/H] trends for each element and then make a brief comparison with studies in the literature on this subject. This comparison is divided into two parts: first, we compare studies on abundances in stars with planets; second, we extend the comparison to other studies regarding abundance trends in metal-rich stars of the Galactic disc. We focus our attention mainly on the [Fe/H] > 0 range. Given the unobserved or probably insignificant differences between the two samples of stars presented, we consider the distribution as a whole for the rest of the analysis. Possible differences between our trends and those recently published could be of great interest since it might reflect the presence of planets. In contrast, any relation to the presence of a planet is perhaps coincidental and the global trends observed are probably best interpreted as a consequence of Galactic chemical evolution.

Table 6. Average abundances ⟨[X/H]⟩ for stars with planets and for comparison sample stars. For each element the rms around the mean and the abundances difference between the two samples (101 and 93 respectively) are also listed.

Species	Planet-hosts		No-hosts		Average
(X)	⟨[X/H]⟩	σ	⟨[X/H]⟩	σ	diff.
Si	0.09	0.20	−0.13	0.24	0.23
Ca	−0.01	0.19	−0.22	0.22	0.22
Ti	0.15	0.17	0.01	0.19	0.14
Sc	0.16	0.20	−0.08	0.24	0.25
V	0.21	0.24	0.08	0.26	0.13
Cr	0.04	0.22	−0.18	0.25	0.22
Mn	0.15	0.33	−0.14	0.33	0.29
Co	0.16	0.25	−0.04	0.26	0.20
Ni	0.09	0.24	−0.17	0.27	0.26
Na	0.12	0.24	−0.17	0.26	0.29
Mg	0.19	0.19	−0.05	0.21	0.23
Al	0.19	0.21	−0.01	0.23	0.18

6.1. The α elements

6.1.1. Silicon

In Figs. 7 and 8 we note a slight [Si/Fe] overabundance compared to the solar value at [Fe/H] $\lesssim -0.2$ (with a rather larger scatter), while the point distribution remains constant at [Si/Fe] ~ 0.0 for the rest of the metallicity range.

Our results agree with the previous chemical analyses of stars with planets by Gonzalez et al. (2000, hereafter GZ00), Bodaghee et al. (2003, hereafter BOD) and Fischer & Valenti (2005). Sadakane et al. (2002, hereafter SD02) in their study analysed only a few objects (12 stars with extrasolar planets) but their abundance distribution is flat at high metallicities.

Edvardsson et al. (1993, hereafter EAGLNT) and Chen et al. (2000, hereafter C00) obtained similar results, as well as Bensby et al. (2003, hereafter BEN) and Fulbright et al. (2002, hereafter FUL) in the range [Fe/H] > 0. In another study on metal-rich stars ([Fe/H] > 0.10) (Felzing & Gustafsson 1998, hereafter FG98) the [Si/Fe] distribution exhibits a constant trend around the solar value. All these results differ from those of Allende Prieto et al. (2004, hereafter AL04), in which the abundance trend for Si changes abruptly around [Fe/H] ~ 0 and assumes a positive slope.

6.1.2. Calcium

Contrary to the other α elements, the [Ca/Fe] ratio seems to decrease quite uniformly (see Figs. 7 and 8). In particular, the plot suggests the presence of a plateau in the range $-0.2 \lesssim$ [Fe/H] $\lesssim 0.2$ followed, for higher metallicities, by a slight fall-off. Planet-host stars with $T_{\rm eff} < 5000$ K show a certain dispersion in [Ca/Fe] values, for example the stars HD 177830, HD 137759 and HD 114783.

The similar behaviour of calcium trends for stars both with and without planets has been observed in other studies of

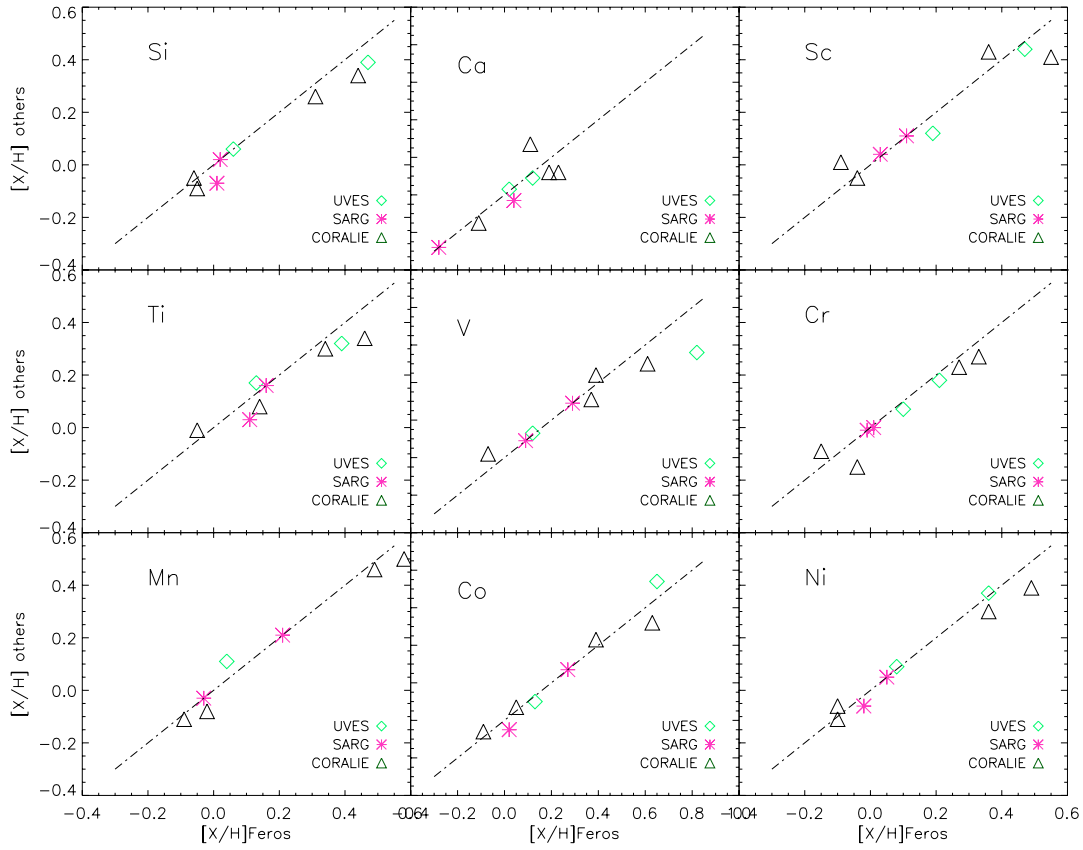

Fig. 4. Comparison of the abundances of nine refractory elements calculated with *EW* values measured from spectra taken with different instruments. Along the *x*-asis are results from FEROS spectra, while along the *y*-axis we represent abundance values for the same objects, calculated using other spectra. UVES, CORALIE and SARG results are respectively represented with rhombi (HD 16141, HD 27442), triangles (HD 83443, HD 92788, HD 106252, HD 114386) and asterisks (HD 114783, HD 147513).

chemical abundances (BOD and GZ00). As BOD have noticed, SD02 analysed only two stars in the range $0.2 \lesssim$ [Fe/H] $\lesssim 0.4$ (where a possible plateau is suggested), so the comparison with our results is only partially valid.

The Ca distribution appears quite "flat" in the data presented by EAGLNT, FG89, AL04 and FUL. However, the results plotted by BEN appear to decrease for [Fe/H] ~ 0.2–0.3.

6.1.3. Titanium

The titanium [Ti/Fe] ratio decreases in the range $-0.6 \lesssim$ [Fe/H] $\lesssim 0$ until the solar value where the distribution settles (Figs. 7 and 8).

Similar trends have been obtained by BOD and Fischer & Valenti (2005), while we cannot observe any slope change around $-0.2 \lesssim$ [Fe/H] $\lesssim 0$ in SD02, because only a few objects have been plotted. Despite the large scatter in the GZ00 data, titanium abundances seem to decrease gradually with metallicity.

A quite pronounced point dispersion is also observed in EAGLNT, BEN and CH00, especially for [Fe/H] $\lesssim -0.3$ (as seen here). This scatter is probably due to the overestimation of *EW*s caused by the increasing blending effect (which becomes severer as $T_{\rm eff}$ falls) or by Galactic evolution effects. Finally, comparing the trends for [Fe/H] > 0 we note that [Ti/Fe] values remain approximately constant in the plots of BEN, FUL and FG98, while the data of AL04 again show a rise above solar metalicity.

6.1.4. Scandium

Figures 7 and 8 illustrate that the scandium trend is similar to that of other α elements. It drops until $-0.2 \lesssim$ [Fe/H] $\lesssim 0$ and afterwards the [Sc/Fe] ratio approximately follows the solar value at high metallicities.

Previous studies on stars with planets have obtained similar results, as presented in BOD and SD02.

There are only a few studies in the literature about scandium abundances. The most detailed one was presented by Nissen et al. (2000) in the range $-1.4 <$ [Fe/H] < 0.1, so comparison with our results at high metallicity is not possible at all. However, it is interesting to note a slope change at [Fe/H] $\sim -0.3, -0.2$ that is also represented in our graphs. Results by FG98 show a substantial star-to-star scatter but globally the [Sc/Fe] ratio remains around solar for [Fe/H] > 0. In contrast, the AL04 plot shows large enrichments in scandium for metal-rich stars.

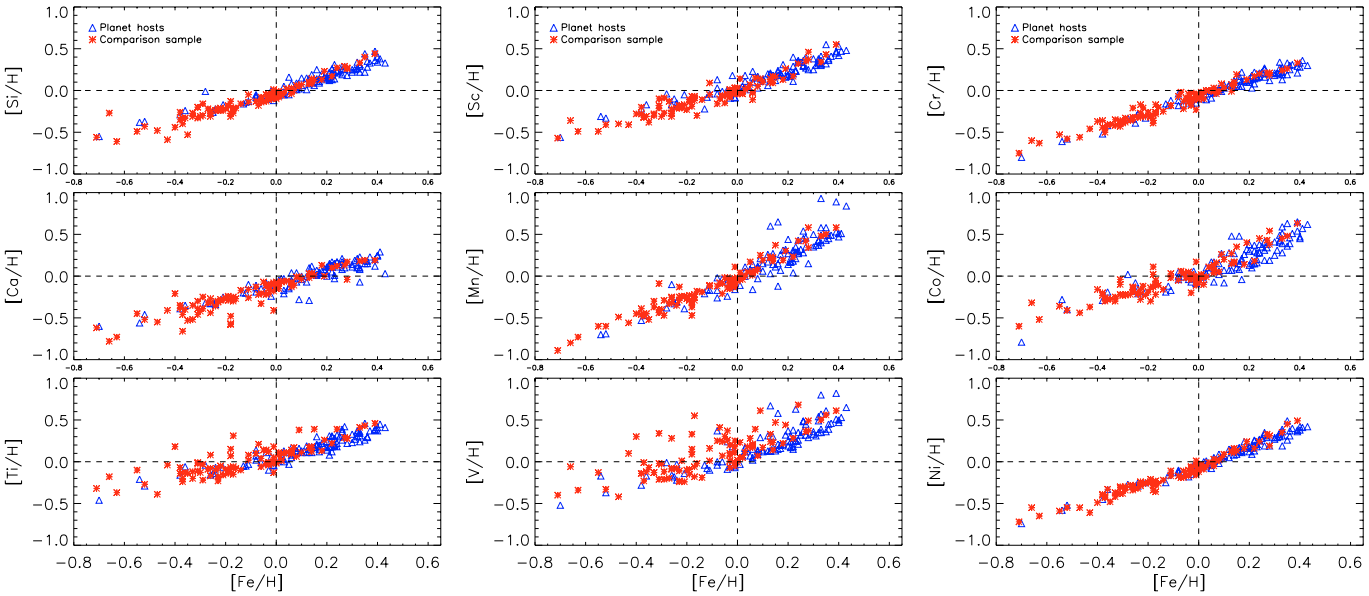

Fig. 5. [*X*/H] vs. [Fe/H] for Si, Ca, Ti (*left*), for Sc, Mn and V (*centre*), for Cr, Co and Ni (*right*). Triangles and asterisks represent stars with planetary-mass companion and "single" field stars, respectively. The intersection of the dotted lines indicates solar value.

6.2. The Fe-group elements

6.2.1. Manganese

Manganese is one of the lesser studied element in the literature. Manganese lines turn out to be the most difficult to measure owing to unknown blended lines that probably cause the quite large point spread, particularly for stars with planets. The [Mn/Fe] ratio generally tends to increase with the metallicity, differently from other iron-peak elements (see Fig. 8). In Fig. 7 we observe a clear change of slope around $-0.2 \lesssim$ [Fe/H] $\lesssim 0$.

Despite a certain scatter, we note the good agreement between our results and those of BOD and SD02.

Nissen et al. (2000) analysed Mn abundances, in disc stars ($-1.4 <$ [Fe/H] < 0.1). These results show an evident increase in manganese abundances for the entire metallicity range considered. Another study (FG98) also exhibits a slight linear [Mn/Fe] dependence on iron in metal-rich stars.

6.2.2. Vanadium

On the subject of vanadium abundances, Fig. 7 (bottom right) clearly shows how removing cooler stars ($T_{\rm eff} < 5000$ K) from the data considerably reduces the dispersion of points. Although vanadium belongs to the iron-peak group, we note that [V/Fe] ratio behaves like an α element. Figure 8 shows that [V/Fe] values in stars with planets are systematically ∼0.10 dex lower than in the comparison sample stars.

Since planet-hosts are, on average, hotter than comparison sample stars (see Fig. 2) and [V/Fe] shows a negative slope with $T_{\rm eff}$, this effect may contribute to the observed difference.

The same considerable scatter is observed in the studies by BOD and SD02, but good agreement among trends is found in both cases. Contrary to our results and those of BOD, SD02 emphasized that the [V/Fe] values of stars with planets are about 0.15 dex higher than comparison sample vanadium abundances. This mismatch could suggest that vanadium analysis is strongly influenced by an NLTE effect, as discussed in Sect. 3.1.

There are not many studies regarding vanadium abundances in metal-rich stars without planets. The [V/Fe] ratio remains around the solar value in the plots of FG98 and CH00, for [Fe/H] > 0.

6.2.3. Chromium

Chromium abundances in our target are constant around [Cr/Fe] ∼ −0.05 dex (see Fig. 8). We note very little scatter for this element (Fig. 7).

Our observed trend is similar to those already published by BOD and SD02: the point distribution is uniform, constant and with little scatter. However, the BOD data show about 0.05 dex systematically lower chromium abundances compared to our results.

Good agreement is found with the FG98, CH00, BEN and FUL plots. All these results exhibit a [Cr/Fe] ratio of around 0.

6.2.4. Cobalt

The [Co/Fe] ratio first decreases to the solar value and then slowly rises for metal-rich stars (see also Fig. 8). The figures also show that the abundances of metal-rich stars with planets seems to be lower (∼0.05 dex) than [Co/Fe] values for stars without planets.

Previous studies of BOD and SD02, have obtained similar results for cobalt. In this last paper authors suggested that planet-host stars exhibit a slight Co overabundance with respect to the solar value (∼0.15 dex) when compared to stars with no companions.

Our results resemble those of FG98, while with respect to AL04 we obtained a change of slope of around [Fe/H] ∼ 0.

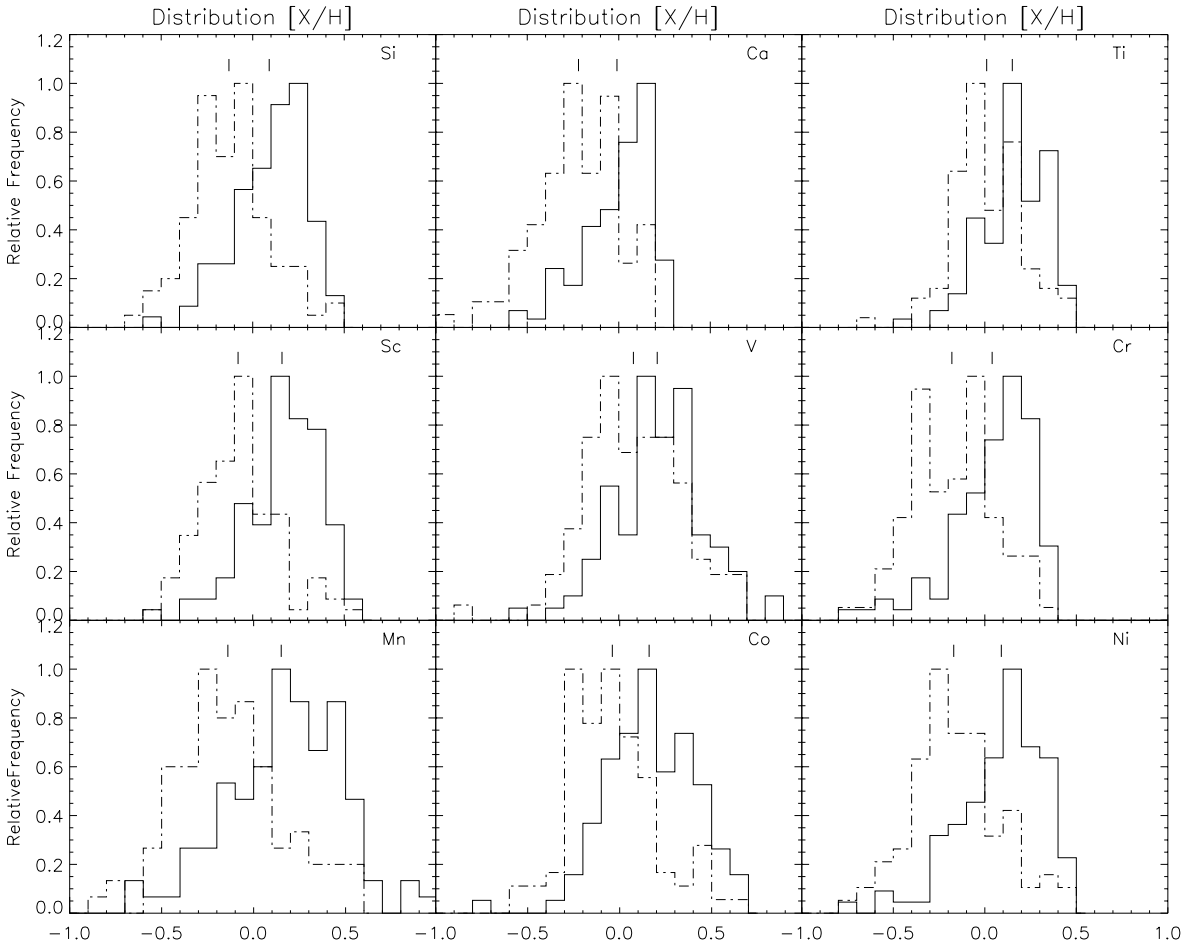

Fig. 6. [*X*/H] distribution for each element. The planet-host stars and the comparison sample are represented with solid and dotted lines, respectively.

6.2.5. Nickel

Similarly to calcium and vanadium, the nickel trend shows a possible plateau in the range $-0.2 \lesssim$ [Fe/H] $\lesssim 0$ and hence a slight slope change for metal-rich stars (see Fig. 7).

Our trends resemble those observed by BOD, SD02 and Fischer & Valenti (2005). The [Ni/Fe] ratio seems to increase slightly in metal-rich stars.

In most of the studies considered (see FG98, CH00, FUL, EAGLNT) nickel abundances exhibit a uniform and approximately constant trend around the solar value. In the results proposed by BEN, nickel abundances remain constant until [Fe/H] ~ 0.2, where the values are greater than the rest of the set of data. A different plot is represented by AL04: the [Ni/Fe] ratio increases for higher metallicity values.

6.3. Na, Mg and Al

In Figs. 10–11 we present the plots for Na, Mg and Al. As discussed in detail in the paper by Beirão et al. (2005), the [Na/Fe] ratio slowly decreases as a function of [Fe/H] until the solar metallicity, then we can observe a change of the slope. This behaviour is similar to that shown by some refractory abundance distribution (e.g. Si, Ti, Sc). Despite the dispersion of the points, the [Na/Fe] values are on average below solar for [Fe/H] ~ 0.0.

The Mg and Al abundances also resemble those derived for Si, Ti, Sc. We note that the decrease in the [Mg/Fe] and [Al/Fe] values with increasing metallicity in the range $-0.70 <$ [Fe/H] < 0 is stronger than for Na. For metal-rich stars the abundance distributions for the three elements stay at approximately solar value except for a light upturn in [Na/Fe] and [Al/Fe] values.

These results agree globally with previous studies of stars with planets (see SD02; GZ00; and Fischer & Valenti 2005, for Na plots) and we also confirm that Mg and Al may be slightly enhanced in the planet-host HD 168746, as noticed in SD02. The [Na/Fe] upturn above solar metallicity is also found in GZ00 and both EAGLNT, FG98, BEN, but not in CH00. With respect to Al abundances, other authors (EAGLNT; FG98; BEN) have observed similar trends. In the plots proposed by CH00 we note a clear upturn at [Fe/H] $\sim -0.2, -0.3$, as traced by comparison stars in our sample.

Possible differences between the abundance trends of the two groups of stars have been observed here only for metal-rich stars. It is particularly interesting to note that comparison stars continue to show a decrease in [Mg/Fe] with

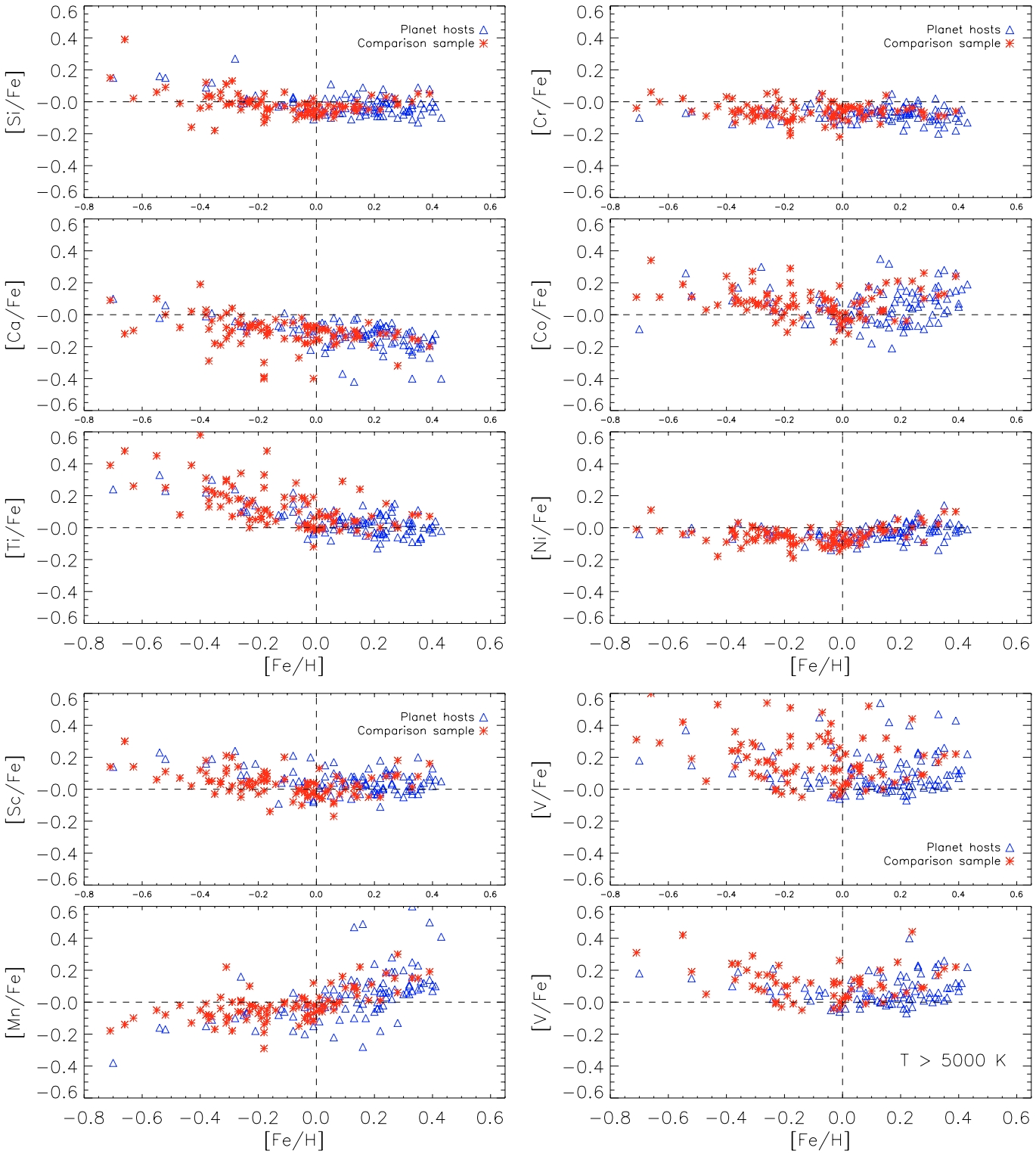

Fig. 7. [*X*/Fe] vs. [Fe/H](in dex) for *α elements* (Si, Ca, Ti, Sc) and for *iron-peak elements* (Cr, Co, Ni, Mn, V). [V/Fe] vs. [Fe/H] for $T_{\rm eff}$ > 5000 K objects only (*below right panel*). The triangles and asterisks represent stars with planets and "single" stars, respectively. The intersection of the dotted lines indicates the solar value.

increasing [Fe/H], while maintaining the slope observed for lower metallicity, while planet-hosts change the slope. An opposite effect is observed for [Al/Fe] where the planet hosts seem to have less Al than their "single" conterparts. The dependence of [Mg/Fe] on $T_{\rm eff}$ is not responsible for this effect (see Figs. 1 and 2 in Beirão et al. 2005) and we cannot rule out that this difference is real. Figure 10 also shows that removing cooler stars ($T_{\rm eff}$ < 5000 K) from the dataset does not change these results. GZ00 also suggested a difference in [Mg/Fe] values between planet-host and single stars.

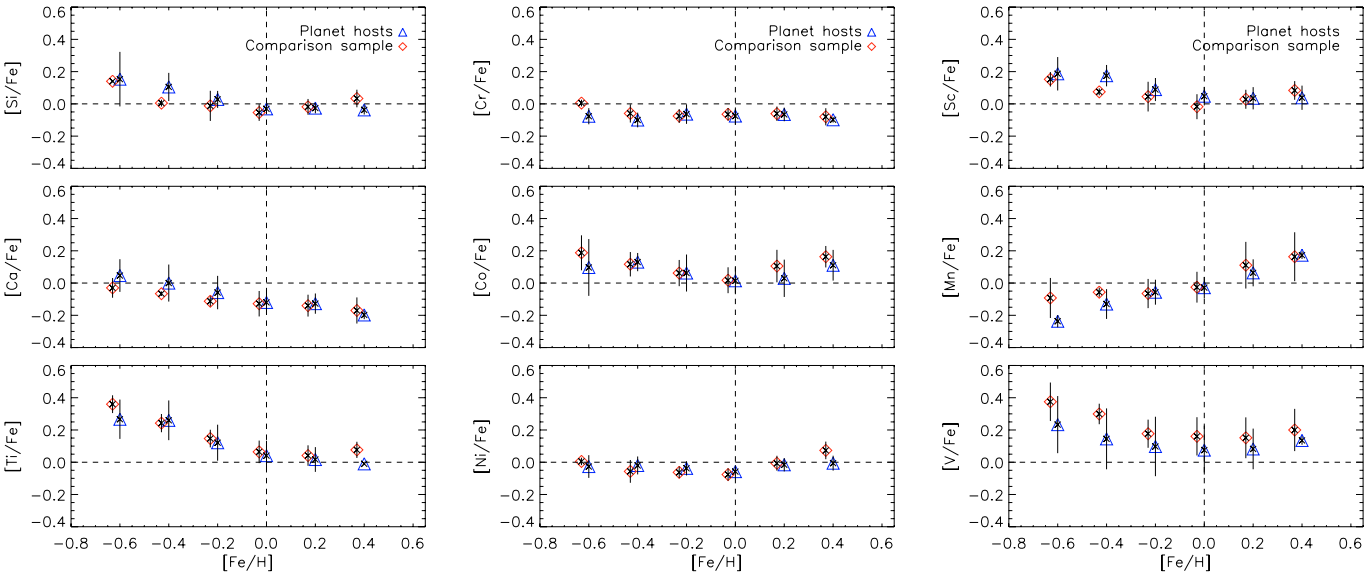

Fig. 8. [*X*/Fe] vs. [Fe/H] trends using binned average values. The bins are 0.2 dex wide, centred on [Fe/H] = −0.6, −0.4, −0.2, 0, 0.2 and 0.4 for both samples. Triangles are planet-hosts while rhombi are stars without a planetary-mass companion. The error bars represent the standard deviation about the mean value.

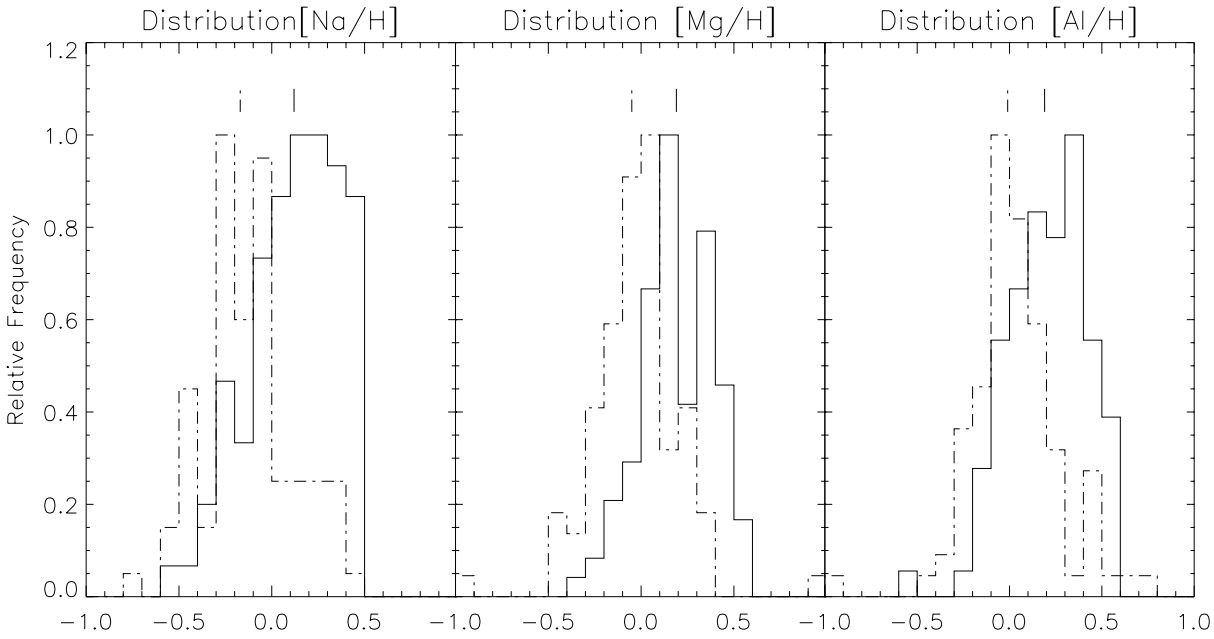

Fig. 9. Same as Fig. 6 but for the Na, Mg and Al distributions.

7. Discussion and conclusion

We have determined abundances for nine refractory elements (other than iron) in a large sample of 101 stars with planets and in a homogeneous comparison sample of 93 stars with no known planets. We have also presented Na, Mg, Al abundances in 52 new comparison sample stars to extend the previous work by Beirão et al. (2005). For each element a uniform and independent study of the two samples was carried out using atmospheric parameters derived from a detailed spectroscopic analysis by Santos et al. (2004a, 2005). Abundance ratios [*X*/H] vs. [Fe/H] and [*X*/Fe] vs. [Fe/H] have been plotted to compare the two samples and to try to find differences eventually connected to the presence of giant planets. This study was also intended to provide a complete comparison in the high metallicity domain, where studies had lacked "single" stars with [Fe/H] > 0.1. Furthermore, the data could provide clues clarifying the chemical evolution of planetary systems.

In our analysis we stressed a certain diversity of trends for elements of a common origin. On one hand not all the refractory elements studied here show the same behaviour; on the other hand, the abundance trends of elements coming from the same nucleosynthesis source are not always alike, in contrast with that we expected.

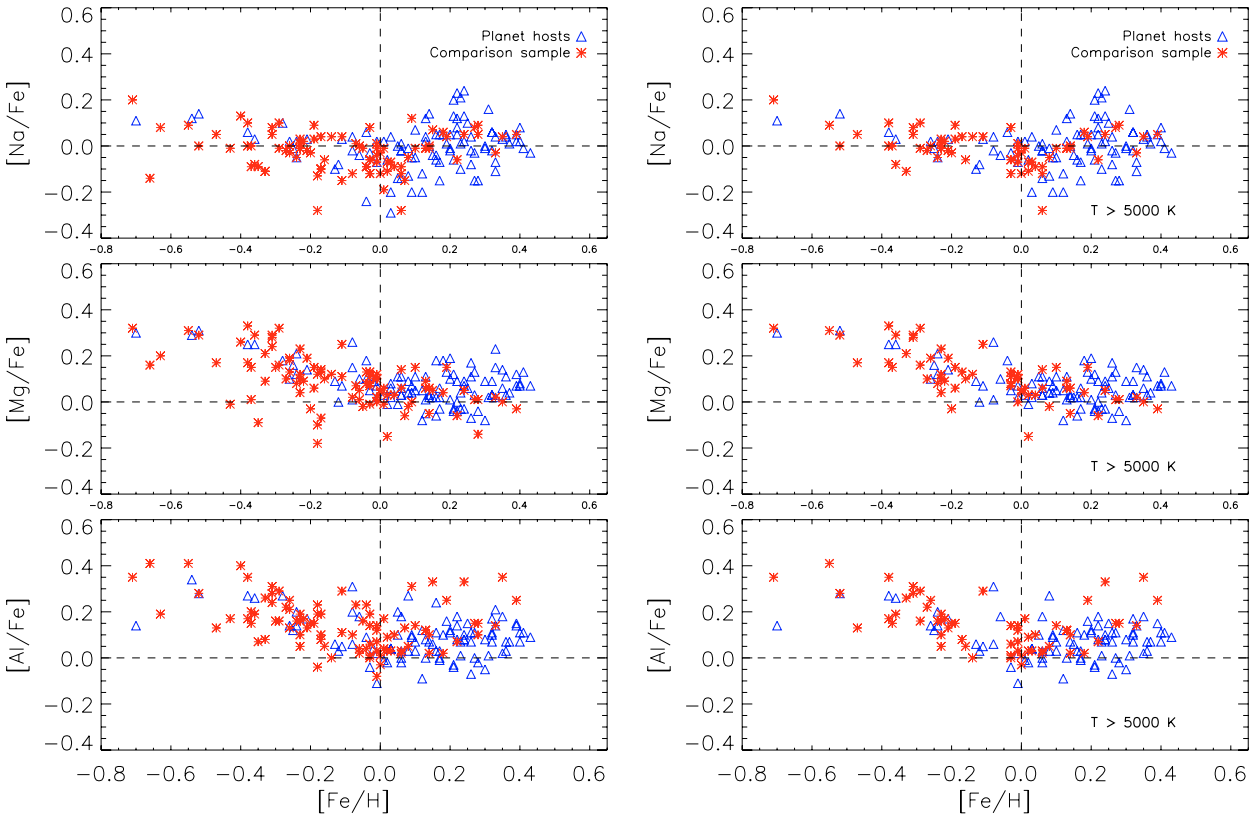

Fig. 10. [*X*/Fe] vs. [Fe/H] (in dex). Results by Beirão et al. (2005) with the addition of abundances from new comparison sample spectra. On the left are the plots for Na, Mg and Al, and on the right the same plots only for $T_{\rm eff}$ > 5000 K objects. Triangles and asterisks represent stars with planetary-mass companions and "single" field stars, respectively. The intersection of the dotted lines indicates the solar value.

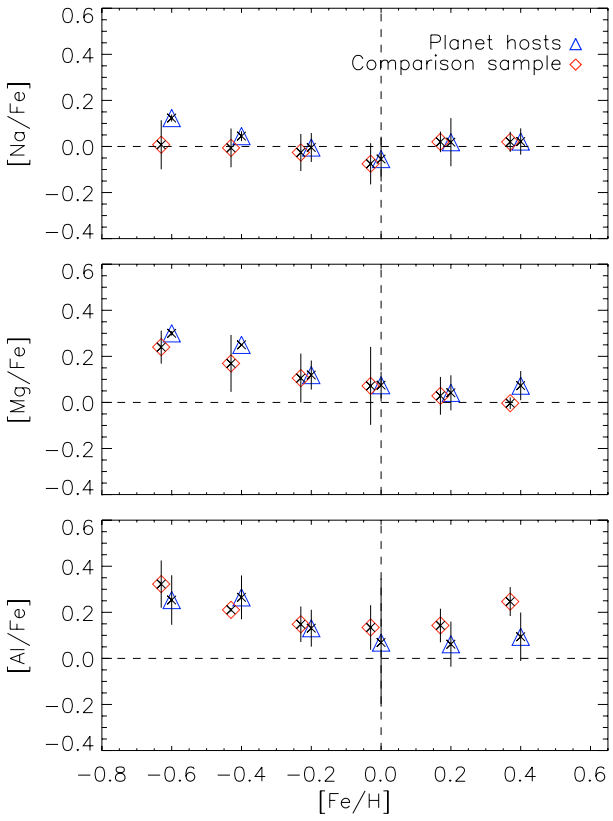

Fig. 11. The same as Fig. 8 but for Na, Mg and Al.

Our concluding remarks are as follows:

- Again we confirm that the excess of metallicity observed for planet hosts is not unique to iron.
- The abundance trends of stars with planets are very similar to those traced by comparison sample stars. This feature could favour the primordial hypothesis to explain the metallicity excess in stars harbouring planets. In any case, some elements (e.g. Mg, Al, V, Co) show certain differences in the behaviour of abundances of stars with planets and "single" stars, in the higher metallicity range. We thus do not exclude the possibility that the presence of a planet might influence the composition of certain elements in the atmosphere of metal rich stars.
- Good agreement was found with both previous published studies on abundances in stars with extrasolar planets and most studies on metal-rich stars of the Galactic disc. One might suggest that the observed trends are simply a conseguence of Galactic chemical evolution, with no particular mechanism linked to the presence of a planet. To this end, only the calcium abundances show a different trend when comparing studies on stars with planets (BOD, GZ00 and this article) and most chemical analysis on Galactic disc stars (EAGLNT, FG98, AL04, FUL).

In the future gathering new homogeneous abundance values of other elements with a wide range of condensation temperatures $T_{\rm C}$ will be of great importance. For example, a detailed

comparison of [*X*/Fe] abundances of volatile and refractory elements is currently in progress . This study will give us the chance to discuss the relative importance of differential accretion (e.g. Gonzalez 1997; Smith et al. 2001; Sadakane et al. 2003) in stars harbouring extrasolar planets.

Acknowledgements. Support from Fundação para a Ciência e a Tecnologia (Portugal) to NCS in the form of a scholarship (reference SFRH/BPD/8116/2002) and a grant (reference POCI/CTE-AST/56453/2004) are gratefully acknowledged. Thanks to the anonymous referee for his/her useful suggestions.

References

Allende Prieto, C., Barklem, P. S., Lambert, D. L., & Cunha, K. 2004, A&A, 420, 183
Anders, E., & Grevesse, N. 1989, Geochim, Cosmochim. Acta, 53, 197
Beirão, P., Santos, N. C., Israelian, G., & Mayor, M. 2005, A&A, 438, 251
Bensby, T., Feltzing, S., & Lundström, I. 2003, A&A, 410, 527 (BEN)
Bensby, T., Feltzing, S., Lundström, I., & Ilyin, I. 2005, A&A, 433, 185
Bodaghee, A., Santos, N. C., Israelian, G., & Mayor, M. 2003, A&A, 404, 717 (BOD)
Deliyannis, C. P., Cunha, K., King, J. R., & Boesgaard, A. M. 2000, AJ, 119, 2437
Desidera, S., Gratton, R. G., Endl, M., Claudi, R. U., & Cosentino, R. 2004, A&A, 420, L27
Chen, Y. Q., Nissen, P. E., Zhao, G., Zhang, H. W., & Benoni, T. 2000, A&AS, 141, 491 (CH00)
Ecuvillon, A., Israelian, G., Santos, N. C., et al. 2004a, A&A, 418, 703
Ecuvillon, A., Israelian, G., Santos, N. C., et al. 2004b, A&A, 426, 619
Ecuvillon, A., Israelian, G., Santos, N. C., et al. 2006, A&A, 445, 633 [arXiv:astro-ph/0509326]
Edvardsson, B., Andersen, J., Gustafsson, B., et al. 1993, A&A, 275, 101 (EAGLNT)
Feltzing, S., & Gustafsson, B. 1998, A&AS, 129, 237 (FZ98)
Fischer, D., & Valenti, J. 2005, ApJ, 622, 1102
Fulbright, J. P. 2002, AJ, 123, 404 (FUL)
García López, R., & Pérez de Taoro, M. R. 1998, A&A, 334, 599
Gray, D. 1992, in The observation and analysis of stellar photospheres (Cambridge Univ. Press)
Gonzalez, G. 1997, MNRAS, 285, 403
Gonzalez, G. 1998, A&A, 334, 221
Gonzalez, G., & Laws, C. 2000, A&A, 119, 390
Gonzalez, G., Laws, C., Tyagi, S., & Reddy, B. 2001, AJ, 121, 432
Gurtovenko, E. A., & Kostyk, R. I. 1989, Fraunoffer spectrum and system of solar oscillator strengths, KiIND, 200
Israelian, G., Santos, N. C., Mayor, M., & Rebolo, R. 2001, Nature, 411, 163
Israelian, G., Santos, N. C., Mayor, M., & Rebolo, R. 2003a, A&A, 405, 753
Israelian, G. 2003b, in IAU S219: Stars as Sun: Activity, Evolution, and Planets, ed A. K. Dupree (San Francisco: ASP)
Israelian, G., Santos, N. C., Mayor, M., & Rebolo, R. 2004, A&A, 414, 601
Kurucz, R. L. 1993, CD-ROMs, ATLAS9 Stellar Atmospheres Programs and 2 km s^{-1} Grid (Cambridge: Smithsonian Astrophys. Obs.)
Kurucz, R. L., Furenlid, I., Brault, J., & Testerman, L. 1984, Solar Flux Atlas from 296 to 1300 nm, NOAO Atlas No. 1
Mayor, M., & Queloz, D. 1995, Nature, 378, 355
McWilliam, A. 1997, ARA&A, 35, 503
Moore, C. E., Minnaert, M. G. J., & Houtgast, J. 1966, The solar Spectrum 2934 Å to 8770 Å
Murray, N., & Chaboyer, B. 2002, 566, 442
Laws, C., & Gonzalez, G. 2001, ApJ, 553, 405
Laws, C., Gonzalez, G., Walker, K. M., et al. 2003, AJ, 125, 2664
Nissen, P. E., Chen, Y. Q., Schuster, W. J., & Zhao, G. 2000, A&A, 353, 722
Pinsonneault, M. H., DePoy, D. L., & Coffee, M. 2001, AJ, 556, L59
Reid, I. N. 2002, PASP, 114, 306
Reddy, B. E., Tomkin, J., Lambert, D. L., & Allend Prieto, C. 2003, MNRAS, 340, 304
Sadakane, K., Ohukubo, M., Takada, Y., et al. 2002, PASJ, 54, 911
Santos, N. C., Israelian, G., & Mayor, M. 2000, A&A, 363, 228
Santos, N. C., Israelian, G., & Mayor, M. 2001a, A&A, 373, 1019
Santos, N. C., Israelian, G., & Mayor, M. 2001b, in Confirming the Metal-Rich Nature of Stars with Giant Planets. Proceedings of the 12th Cambridge workshop Cool Stars, Stellar System, and the Sun, Boulder, Colorado, USA
Santos, N. C., García López R. J., Israelian, G., et al. 2002, A&A, 386, 1028
Santos, N. C., Israelian, G., Mayor, M., Rebolo, R., & Udry, S. 2003, A&A, 398, 363
Santos, N. C., Israelian, G., & Mayor, M. 2004a, A&A, 415, 1153
Santos, N. C., Israelian, G., García López, R., et al. 2004b, A&A, 427, 1085
Santos, N. C., Israelian, G., Mayor, M., et al. 2005, A&A, 437, 1127
Smith, V. V., Cunha, C., & Lazzaro, D. 2001, AJ, 121, 3207
Sneden, C. 1973, Ph.D. Thesis, University of Texas
Lewis, J. S. 1995, in Physics and Chemistry of the Solar System (San Diego: Academic Press)
Thévenin, F., & Idiart, T. P. 1999, ApJ, 521, 753
Takeda, Y., Sato, B., Kambe, E., et al. 2001, PASJ, 53, 1211
Thielemann, K.-F., Argast, D., Brachwitz, F., et al. 2002, A&SS, 281, 25
Timmers, F. X., Woosley, S. E., & Weaver, T. A. 1995, ApJS, 98, 617
Vauclair, S. 2003, ApJ, 605, 874

Online Material

Table 7. Stars with giant planets and abundances derived for Si, Ca, Sc, Ti, V, Cr, Mn, Co, Ni.

Star (HD)	[Si/H]	[Ca/H]	[Sc/H]	[Ti/H]	[V/H]	[Cr/H]	[Mn/H]	[Co/H]	[Ni/H]
HD 142	0.19 ± 0.05	0.12 ± 0.13	0.18 ± 0.12	0.18 ± 0.15	0.30 ± 0.12	0.12 ± 0.09	0.14 ± 0.08	0.27 ± 0.05	0.15 ± 0.12
HD 1237	0.01 ± 0.06	0.00 ± 0.10	0.06 ± 0.11	0.11 ± 0.08	0.13 ± 0.12	0.06 ± 0.06	0.17 ± 0.07	0.07 ± 0.09	0.05 ± 0.04
HD 2039	0.34 ± 0.04	0.21 ± 0.11	0.38 ± 0.13	0.37 ± 0.07	0.49 ± 0.10	0.34 ± 0.11	0.43 ± 0.10	0.43 ± 0.09	0.35 ± 0.07
HD 3651	0.15 ± 0.07	−0.07 ± 0.14	0.20 ± 0.10	0.19 ± 0.07	0.31 ± 0.13	0.07 ± 0.04	0.26 ± 0.11	0.28 ± 0.05	0.15 ± 0.07
HD 4203	0.40 ± 0.06	0.24 ± 0.09	0.53 ± 0.12	0.41 ± 0.08	0.47 ± 0.10	0.33 ± 0.08	0.47 ± 0.13	0.47 ± 0.06	0.42 ± 0.08
HD 4208	−0.23 ± 0.06	−0.31 ± 0.09	−0.15 ± 0.08	−0.14 ± 0.06	−0.22 ± 0.08	−0.28 ± 0.05	−0.3 ± 0.05	−0.21 ± 0.06	−0.25 ± 0.07
HD 6434	−0.37 ± 0.06	−0.46 ± 0.12	−0.33 ± 0.12	−0.29 ± 0.11	−0.37 ± 0.10	−0.58 ± 0.06	−0.69 ± 0.10	−0.40 ± 0.10	−0.52 ± 0.06
HD 8574	0.01 ± 0.08	0.04 ± 0.08	0.16 ± 0.10	0.05 ± 0.07	0.02 ± 0.09	−0.02 ± 0.08	−0.16 ± 0.10	−0.07 ± 0.14	0.00 ± 0.07
HD 9826	0.14 ± 0.06	0.10 ± 0.09	0.21 ± 0.13	0.15 ± 0.09	0.13 ± 0.07	0.05 ± 0.06	0.03 ± 0.14	0.07 ± 0.07	0.15 ± 0.10
HD 10647	−0.09 ± 0.04	−0.10 ± 0.05	−0.09 ± 0.06	−0.10 ± 0.04	−0.06 ± 0.15	−0.15 ± 0.06	−0.12 ± 0.08	−0.07 ± 0.03	−0.15 ± 0.05
HD 10697	0.09 ± 0.03	0.03 ± 0.07	0.18 ± 0.09	0.11 ± 0.04	0.17 ± 0.05	0.04 ± 0.04	0.27 ± 0.17	0.17 ± 0.06	0.08 ± 0.05
HD 12661	0.28 ± 0.06	0.15 ± 0.13	0.38 ± 0.09	0.29 ± 0.05	0.39 ± 0.09	0.25 ± 0.07	0.45 ± 0.09	0.46 ± 0.06	0.31 ± 0.07
HD 13445	−0.22 ± 0.06	−0.34 ± 0.11	−0.19 ± 0.10	−0.07 ± 0.09	−0.03 ± 0.10	−0.28 ± 0.05	−0.31 ± 0.06	−0.16 ± 0.06	−0.29 ± 0.05
HD 16141	0.06 ± 0.05	0.03 ± 0.09	0.12 ± 0.07	0.17 ± 0.06	0.13 ± 0.05	0.07 ± 0.06	0.11 ± 0.05	0.10 ± 0.04	0.09 ± 0.05
HD 17051	0.19 ± 0.05	0.17 ± 0.11	0.29 ± 0.08	0.26 ± 0.07	0.37 ± 0.12	0.16 ± 0.07	0.28 ± 0.10	0.19 ± 0.11	0.19 ± 0.06
HD 19994	0.23 ± 0.08	0.17 ± 0.08	0.36 ± 0.07	0.18 ± 0.07	0.26 ± 0.15	0.20 ± 0.04	0.43 ± 0.05	0.28 ± 0.08	0.27 ± 0.08
HD 20367	0.11 ± 0.08	0.04 ± 0.12	0.20 ± 0.13	0.15 ± 0.12	0.16 ± 0.13	0.22 ± 0.09	0.07 ± 0.14	−0.04 ± 0.15	0.11 ± 0.09
HD 22049	−0.16 ± 0.05	−0.20 ± 0.14	−0.22 ± 0.11	−0.05 ± 0.07	−0.04 ± 0.08	−0.16 ± 0.05	−0.21 ± 0.07	−0.19 ± 0.07	−0.25 ± 0.06
HD 23079	−0.13 ± 0.06	−0.10 ± 0.08	−0.04 ± 0.12	−0.03 ± 0.08	−0.10 ± 0.09	−0.12 ± 0.07	−0.17 ± 0.13	−0.17 ± 0.13	−0.13 ± 0.07
HD 23596	0.25 ± 0.05	0.19 ± 0.06	0.30 ± 0.05	0.27 ± 0.06	0.31 ± 0.07	0.20 ± 0.05	0.37 ± 0.08	0.31 ± 0.07	0.29 ± 0.07
HD 27442	0.47 ± 0.15	0.12 ± 0.17	0.47 ± 0.15	0.39 ± 0.19	0.82 ± 0.19	0.21 ± 0.13	0.89 ± 0.08	0.65 ± 0.15	0.36 ± 0.10
HD 28185	0.18 ± 0.06	0.05 ± 0.08	0.29 ± 0.11	0.31 ± 0.08	0.15 ± 0.06	0.15 ± 0.04	0.28 ± 0.09	0.30 ± 0.07	0.25 ± 0.04
HD 30177	0.36 ± 0.07	0.20 ± 0.13	0.45 ± 0.07	0.38 ± 0.12	0.51 ± 0.12	0.29 ± 0.07	0.53 ± 0.10	0.54 ± 0.10	0.38 ± 0.06
HD 33636[b]	−0.08 ± 0.08	−0.19 ± 0.09	0.03 ± 0.07	0.02 ± 0.13	−0.04 ± 0.07	−0.12 ± 0.07	−0.17 ± 0.09	−0.04 ± 0.11	−0.13 ± 0.09
HD 37124[b]	−0.29 ± 0.08	−0.39 ± 0.09	−0.22 ± 0.10	−0.16 ± 0.06	−0.28 ± 0.11	−0.52 ± 0.07	−0.53 ± 0.08	−0.29 ± 0.05	−0.45 ± 0.05
HD 38529	0.34 ± 0.06	0.25 ± 0.06	0.42 ± 0.08	0.37 ± 0.07	0.50 ± 0.10	0.28 ± 0.08	0.51 ± 0.17	0.45 ± 0.08	0.38 ± 0.07
HD 39091	0.15 ± 0.04	0.00 ± 0.07	0.14 ± 0.09	0.13 ± 0.06	0.12 ± 0.08	0.03 ± 0.03	0.06 ± 0.06	0.07 ± 0.05	0.07 ± 0.05
HD 40979	0.22 ± 0.05	0.15 ± 0.07	0.18 ± 0.10	0.18 ± 0.06	0.24 ± 0.13	0.18 ± 0.10	0.17 ± 0.16	0.10 ± 0.11	0.16 ± 0.08
HD 46375	0.15 ± 0.06	0.00 ± 0.12	0.17 ± 0.11	0.24 ± 0.09	0.37 ± 0.11	0.12 ± 0.06	0.44 ± 0.13	0.38 ± 0.13	0.17 ± 0.07
HD 47536	−0.38 ± 0.07	−0.56 ± 0.16	−0.31 ± 0.15	−0.21 ± 0.16	−0.17 ± 0.19	−0.61 ± 0.10	−0.70 ± 0.09	−0.28 ± 0.13	−0.58 ± 0.10
HD 49674	0.22 ± 0.05	0.10 ± 0.14	0.30 ± 0.07	0.24 ± 0.09	0.35 ± 0.09	0.19 ± 0.06	0.40 ± 0.05	0.28 ± 0.09	0.19 ± 0.13
HD 50554	−0.06 ± 0.06	−0.05 ± 0.07	0.02 ± 0.08	0.01 ± 0.05	−0.03 ± 0.08	−0.10 ± 0.06	−0.11 ± 0.08	−0.01 ± 0.14	−0.07 ± 0.04
HD 52265	0.22 ± 0.04	0.15 ± 0.06	0.24 ± 0.08	0.19 ± 0.06	0.25 ± 0.13	0.16 ± 0.08	0.21 ± 0.12	0.20 ± 0.09	0.21 ± 0.05
HD 65216	−0.14 ± 0.07	−0.20 ± 0.08	−0.08 ± 0.08	−0.05 ± 0.05	−0.08 ± 0.07	−0.18 ± 0.03	−0.16 ± 0.05	−0.12 ± 0.08	−0.16 ± 0.04
HD 68988	0.35 ± 0.11	0.18 ± 0.14	0.36 ± 0.15	0.30 ± 0.14	0.45 ± 0.07	0.30 ± 0.06	0.49 ± 0.06	0.39 ± 0.11	0.37 ± 0.08
HD 70642	0.20 ± 0.04	0.06 ± 0.07	0.31 ± 0.12	0.22 ± 0.05	0.21 ± 0.08	0.12 ± 0.05	0.31 ± 0.07	0.26 ± 0.05	0.24 ± 0.04
HD 72659	0.05 ± 0.08	−0.03 ± 0.07	0.11 ± 0.09	0.13 ± 0.11	0.17 ± 0.11	−0.01 ± 0.04	0.00 ± 0.09	0.03 ± 0.08	0.01 ± 0.05
HD 73256	0.25 ± 0.06	0.21 ± 0.10	0.30 ± 0.12	0.39 ± 0.09	0.48 ± 0.11	0.27 ± 0.06	0.45 ± 0.13	0.31 ± 0.08	0.33 ± 0.06
HD 73526	0.29 ± 0.05	0.17 ± 0.10	0.40 ± 0.08	0.42 ± 0.08	0.45 ± 0.08	0.21 ± 0.06	0.35 ± 0.10	0.38 ± 0.05	0.31 ± 0.06
HD 74156	0.14 ± 0.04	0.07 ± 0.09	0.22 ± 0.11	0.19 ± 0.07	0.21 ± 0.08	0.05 ± 0.06	0.15 ± 0.10	0.15 ± 0.06	0.16 ± 0.07
HD 75289	0.18 ± 0.06	0.16 ± 0.08	0.25 ± 0.11	0.22 ± 0.06	0.29 ± 0.09	0.12 ± 0.05	0.15 ± 0.10	0.19 ± 0.09	0.19 ± 0.05
HD 75732	0.29 ± 0.07	0.08 ± 0.14	0.32 ± 0.13	0.36 ± 0.12	0.57 ± 0.14	0.22 ± 0.06	0.58 ± 0.13	0.51 ± 0.07	0.31 ± 0.10
HD 76700	0.38 ± 0.03	0.29 ± 0.10	0.47 ± 0.08	0.45 ± 0.05	0.53 ± 0.08	0.36 ± 0.08	0.51 ± 0.12	0.57 ± 0.10	0.41 ± 0.06
HD 80606	0.27 ± 0.06	0.10 ± 0.15	0.34 ± 0.13	0.35 ± 0.10	0.54 ± 0.12	0.27 ± 0.07	0.42 ± 0.16	0.49 ± 0.09	0.33 ± 0.08
HD 82943	0.25 ± 0.05	0.14 ± 0.06	0.25 ± 0.06	0.23 ± 0.06	0.33 ± 0.08	0.18 ± 0.03	0.35 ± 0.08	0.25 ± 0.06	0.27 ± 0.04
HD 83443	0.44 ± 0.06	0.19 ± 0.12	0.55 ± 0.11	0.46 ± 0.10	0.61 ± 0.12	0.33 ± 0.08	0.58 ± 0.16	0.63 ± 0.09	0.49 ± 0.07
HD 89744	0.21 ± 0.05	0.17 ± 0.08	0.20 ± 0.09	0.18 ± 0.06	0.18 ± 0.10	0.14 ± 0.04	0.04 ± 0.13	0.15 ± 0.05	0.20 ± 0.09
HD 92788	0.31 ± 0.04	0.23 ± 0.09	0.36 ± 0.06	0.34 ± 0.07	0.39 ± 0.08	0.27 ± 0.06	0.49 ± 0.10	0.39 ± 0.07	0.36 ± 0.04
HD 95128	0.01 ± 0.03	−0.07 ± 0.08	0.10 ± 0.08	0.08 ± 0.06	0.05 ± 0.06	−0.03 ± 0.04	0.04 ± 0.06	0.09 ± 0.08	0.02 ± 0.06
HD 104985	−0.01 ± 0.08	−0.32 ± 0.12	−0.04 ± 0.09	−0.04 ± 0.11	−0.01 ± 0.13	−0.33 ± 0.10	−0.38 ± 0.13	0.02 ± 0.12	−0.27 ± 0.08
HD 106252	−0.06 ± 0.05	−0.11 ± 0.05	−0.09 ± 0.09	−0.05 ± 0.05	−0.07 ± 0.08	−0.15 ± 0.04	−0.09 ± 0.10	−0.09 ± 0.08	−0.10 ± 0.04
HD 108147	0.13 ± 0.05	0.11 ± 0.09	0.19 ± 0.09	0.14 ± 0.07	0.19 ± 0.07	0.14 ± 0.06	0.14 ± 0.11	0.13 ± 0.05	0.12 ± 0.06
HD 108874	0.14 ± 0.04	0.01 ± 0.10	0.23 ± 0.11	0.20 ± 0.07	0.25 ± 0.09	0.15 ± 0.06	0.35 ± 0.14	0.28 ± 0.09	0.18 ± 0.08
HD 111232	−0.24 ± 0.07	−0.35 ± 0.09	−0.17 ± 0.11	−0.06 ± 0.06	−0.17 ± 0.08	−0.42 ± 0.05	−0.47 ± 0.09	−0.19 ± 0.05	−0.33 ± 0.04
HD 114386	−0.05 ± 0.08	−0.11 ± 0.16	−0.04 ± 0.17	0.14 ± 0.11	0.37 ± 0.14	−0.04 ± 0.09	−0.02 ± 0.08	0.05 ± 0.09	−0.10 ± 0.05
HD 114729	−0.26 ± 0.05	−0.32 ± 0.08	−0.10 ± 0.10	−0.14 ± 0.05	−0.18 ± 0.09	−0.39 ± 0.09	−0.33 ± 0.13	−0.08 ± 0.08	−0.29 ± 0.05
HD 114762[b]	−0.55 ± 0.04	−0.60 ± 0.07	−0.56 ± 0.08	−0.46 ± 0.07	−0.52 ± 0.04	−0.80 ± 0.07	−1.08 ± 0.08	−0.79 ± 0.03	−0.74 ± 0.04

Table 7. continued.

Star (HD)	[Si/H]	[Ca/H]	[Sc/H]	[Ti/H]	[V/H]	[Cr/H]	[Mn/H]	[Co/H]	[Ni/H]
HD 114783	0.02 ± 0.06	−0.28 ± 0.07	0.11 ± 0.08	0.16 ± 0.08	0.29 ± 0.10	−0.01 ± 0.04	0.21 ± 0.06	0.27 ± 0.10	0.05 ± 0.09
HD 117176	−0.12 ± 0.07	−0.15 ± 0.06	−0.01 ± 0.09	−0.01 ± 0.05	0.00 ± 0.07	−0.16 ± 0.03	−0.03 ± 0.05	−0.01 ± 0.05	−0.12 ± 0.05
HD 120136	0.31 ± 0.09	−0.03 ± 0.11	0.23 ± 0.10	0.28 ± 0.12	0.63 ± 0.07	0.17 ± 0.07	0.29 ± 0.06	0.16 ± 0.06	0.21 ± 0.18
HD 121504	0.11 ± 0.04	0.02 ± 0.09	0.18 ± 0.11	0.21 ± 0.06	0.15 ± 0.08	0.13 ± 0.08	−0.12 ± 0.06	0.08 ± 0.07	0.12 ± 0.07
HD 128311	−0.03 ± 0.07	−0.21 ± 0.14	0.18 ± 0.14	0.00 ± 0.12	0.16 ± 0.15	−0.11 ± 0.09	0.06 ± 0.07	0.03 ± 0.07	−0.06 ± 0.07
HD 130322	−0.05 ± 0.06	−0.17 ± 0.14	0.04 ± 0.09	0.03 ± 0.06	0.12 ± 0.07	−0.04 ± 0.04	0.11 ± 0.06	0.10 ± 0.08	−0.03 ± 0.07
HD 134987	0.22 ± 0.07	0.11 ± 0.09	0.38 ± 0.07	0.33 ± 0.08	0.36 ± 0.05	0.21 ± 0.05	0.50 ± 0.11	0.41 ± 0.07	0.29 ± 0.06
HD 136118[b]	−0.10 ± 0.07	−0.08 ± 0.10	−0.02 ± 0.09	−0.01 ± 0.10	−0.09 ± 0.04	−0.09 ± 0.07	−0.24 ± 0.04	−0.04 ± 0.03	−0.11 ± 0.04
HD 137759	0.10 ± 0.09	−0.29 ± 0.14	0.19 ± 0.19	0.18 ± 0.18	0.67 ± 0.17	0.07 ± 0.11	0.60 ± 0.07	0.48 ± 0.16	0.12 ± 0.09
HD 141937	0.06 ± 0.04	−0.04 ± 0.07	0.13 ± 0.10	0.11 ± 0.05	0.14 ± 0.08	0.07 ± 0.05	0.15 ± 0.08	−0.08 ± 0.05	0.07 ± 0.05
HD 142415	0.15 ± 0.05	0.13 ± 0.07	0.23 ± 0.09	0.31 ± 0.07	0.31 ± 0.12	0.18 ± 0.05	0.21 ± 0.08	0.19 ± 0.11	0.18 ± 0.07
HD 143761	−0.17 ± 0.03	−0.25 ± 0.09	−0.05 ± 0.09	−0.07 ± 0.07	−0.14 ± 0.03	−0.33 ± 0.03	−0.39 ± 0.09	−0.19 ± 0.06	−0.25 ± 0.06
HD 145675	0.33 ± 0.06	0.03 ± 0.17	0.48 ± 0.11	0.41 ± 0.13	0.65 ± 0.16	0.30 ± 0.07	0.84 ± 0.09	0.62 ± 0.11	0.42 ± 0.09
HD 147513	0.01 ± 0.06	0.04 ± 0.07	0.03 ± 0.06	0.11 ± 0.07	0.09 ± 0.08	0.01 ± 0.04	−0.03 ± 0.06	0.02 ± 0.05	−0.02 ± 0.04
HD 150706	−0.12 ± 0.04	−0.13 ± 0.07	−0.08 ± 0.07	−0.04 ± 0.05	−0.05 ± 0.04	−0.09 ± 0.03	−0.16 ± 0.04	−0.08 ± 0.07	−0.07 ± 0.04
HD 160691	0.26 ± 0.04	0.13 ± 0.07	0.32 ± 0.04	0.30 ± 0.05	0.35 ± 0.07	0.21 ± 0.05	0.37 ± 0.09	0.41 ± 0.06	0.30 ± 0.04
HD 162020[b]	−0.10 ± 0.09	−0.16 ± 0.16	0.01 ± 0.12	0.11 ± 0.14	0.24 ± 0.16	−0.12 ± 0.09	−0.07 ± 0.09	0.00 ± 0.09	−0.18 ± 0.07
HD 168443	0.08 ± 0.06	−0.05 ± 0.10	0.23 ± 0.08	0.17 ± 0.05	0.15 ± 0.07	0.00 ± 0.04	0.14 ± 0.10	0.17 ± 0.08	0.05 ± 0.05
HD 168746	−0.06 ± 0.06	−0.14 ± 0.11	0.13 ± 0.16	0.07 ± 0.05	0.00 ± 0.13	−0.18 ± 0.05	−0.26 ± 0.02	0.00 ± 0.10	−0.12 ± 0.06
HD 169830	0.12 ± 0.05	0.11 ± 0.07	0.18 ± 0.07	0.08 ± 0.04	0.17 ± 0.13	0.03 ± 0.03	0.17 ± 0.10	0.15 ± 0.08	0.09 ± 0.05
HD 177830	0.31 ± 0.06	−0.07 ± 0.09	0.41 ± 0.12	0.31 ± 0.12	0.80 ± 0.17	0.13 ± 0.07	0.93 ± 0.08	0.59 ± 0.15	0.39 ± 0.09
HD 178911B	0.26 ± 0.06	0.10 ± 0.10	0.27 ± 0.05	0.31 ± 0.07	0.32 ± 0.09	0.20 ± 0.05	0.46 ± 0.15	0.34 ± 0.05	0.29 ± 0.06
HD 179949	0.13 ± 0.05	0.11 ± 0.07	0.11 ± 0.08	0.12 ± 0.05	0.28 ± 0.10	0.08 ± 0.04	0.18 ± 0.08	0.15 ± 0.04	0.13 ± 0.06
HD 186427	0.04 ± 0.05	−0.07 ± 0.10	0.17 ± 0.08	0.13 ± 0.07	0.14 ± 0.06	0.01 ± 0.04	0.10 ± 0.04	0.15 ± 0.05	0.09 ± 0.07
HD 187123	0.08 ± 0.04	0.02 ± 0.08	0.19 ± 0.07	0.12 ± 0.06	0.13 ± 0.04	0.07 ± 0.03	0.23 ± 0.09	0.16 ± 0.03	0.15 ± 0.06
HD 190228	−0.27 ± 0.04	−0.33 ± 0.07	−0.17 ± 0.09	−0.16 ± 0.05	−0.16 ± 0.05	−0.34 ± 0.04	−0.10 ± 0.20	−0.18 ± 0.09	−0.29 ± 0.05
HD 190360A	0.24 ± 0.05	0.11 ± 0.10	0.34 ± 0.09	0.32 ± 0.06	0.35 ± 0.11	0.17 ± 0.06	0.30 ± 0.11	0.38 ± 0.08	0.25 ± 0.06
HD 192263	0.00 ± 0.08	−0.24 ± 0.13	0.18 ± 0.13	0.06 ± 0.10	0.18 ± 0.13	−0.10 ± 0.07	−0.04 ± 0.11	0.06 ± 0.09	−0.04 ± 0.08
HD 195019A	0.09 ± 0.05	−0.03 ± 0.10	0.15 ± 0.09	0.13 ± 0.06	0.12 ± 0.06	0.03 ± 0.06	0.12 ± 0.05	0.06 ± 0.06	0.03 ± 0.04
HD 196050	0.26 ± 0.05	0.13 ± 0.09	0.40 ± 0.09	0.30 ± 0.06	0.38 ± 0.06	0.22 ± 0.09	0.31 ± 0.05	0.37 ± 0.07	0.26 ± 0.07
HD 202206[b]	0.22 ± 0.04	0.15 ± 0.08	0.32 ± 0.06	0.26 ± 0.07	0.36 ± 0.10	0.19 ± 0.05	0.43 ± 0.11	0.36 ± 0.07	0.26 ± 0.05
HD 209458	−0.03 ± 0.05	−0.03 ± 0.06	0.05 ± 0.07	0.04 ± 0.04	0.07 ± 0.07	–	0.00 ± 0.02	−0.04 ± 0.03	0.00 ± 0.05
HD 210277	0.16 ± 0.04	0.08 ± 0.11	0.16 ± 0.11	0.24 ± 0.05	0.32 ± 0.10	0.10 ± 0.05	0.32 ± 0.10	0.32 ± 0.08	0.16 ± 0.05
HD 213240	0.09 ± 0.04	0.04 ± 0.05	0.21 ± 0.09	0.12 ± 0.05	0.20 ± 0.08	0.05 ± 0.07	0.20 ± 0.11	0.18 ± 0.07	0.13 ± 0.04
HD 216435	0.24 ± 0.03	0.17 ± 0.05	0.34 ± 0.06	0.22 ± 0.06	0.21 ± 0.12	0.21 ± 0.06	0.27 ± 0.11	0.28 ± 0.10	0.26 ± 0.06
HD 216437	0.21 ± 0.06	0.14 ± 0.08	0.34 ± 0.09	0.30 ± 0.04	0.32 ± 0.05	0.22 ± 0.06	0.32 ± 0.08	0.35 ± 0.03	0.28 ± 0.05
HD 216770	0.29 ± 0.07	0.08 ± 0.14	0.36 ± 0.06	0.36 ± 0.08	0.49 ± 0.08	0.25 ± 0.06	0.54 ± 0.08	0.41 ± 0.09	0.35 ± 0.07
HD 217014	0.17 ± 0.06	0.03 ± 0.07	0.24 ± 0.10	0.17 ± 0.06	0.25 ± 0.06	0.10 ± 0.03	0.27 ± 0.06	0.30 ± 0.04	0.18 ± 0.04
HD 217107	0.33 ± 0.04	0.23 ± 0.10	0.41 ± 0.07	0.37 ± 0.07	0.46 ± 0.11	0.31 ± 0.07	0.49 ± 0.12	0.51 ± 0.09	0.40 ± 0.06
HD 219449	0.16 ± 0.48	−0.15 ± 0.15	0.07 ± 0.14	0.11 ± 0.18	0.28 ± 0.20	−0.01 ± 0.14	0.17 ± 0.17	0.17 ± 0.14	−0.04 ± 0.10
HD 219542B	0.14 ± 0.03	0.04 ± 0.08	0.20 ± 0.07	0.20 ± 0.07	0.20 ± 0.05	0.11 ± 0.04	0.26 ± 0.06	0.21 ± 0.05	0.13 ± 0.03
HD 222404	0.25 ± 0.12	0.01 ± 0.14	0.24 ± 0.11	0.30 ± 0.12	0.58 ± 0.18	0.17 ± 0.10	0.65 ± 0.06	0.48 ± 0.12	0.17 ± 0.07
HD 222582	−0.05 ± 0.06	−0.13 ± 0.11	0.01 ± 0.10	−0.03 ± 0.10	0.07 ± 0.07	−0.09 ± 0.05	0.08 ± 0.07	0.11 ± 0.10	−0.08 ± 0.12

[b] The companions to these stars have minimum masses above 10 $M_{\rm Jup}$, and are probably Brown-Dwarfs.

Table 8. Stars without giant planets and abundances derived for Si, Ca, Sc, Ti, V, Cr, Mn, Co, Ni.

Star (HD)	[Si/H]	[Ca/H]	[Sc/H]	[Ti/H]	[V/H]	[Cr/H]	[Mn/H]	[Co/H]	[Ni/H]
HD 1581	−0.16 ± 0.05	−0.17 ± 0.07	−0.11 ± 0.07	−0.10 ± 0.07	−0.19 ± 0.09	−0.25 ± 0.04	−0.19 ± 0.11	−0.16 ± 0.12	−0.22 ± 0.06
HD 4391	−0.11 ± 0.08	−0.15 ± 0.11	0.01 ± 0.11	−0.01 ± 0.06	0.01 ± 0.09	−0.18 ± 0.09	−0.11 ± 0.12	0.02 ± 0.08	−0.12 ± 0.06
HD 5133	−0.21 ± 0.08	−0.30 ± 0.12	−0.07 ± 0.12	−0.06 ± 0.10	−0.06 ± 0.15	−0.26 ± 0.07	−0.22 ± 0.10	−0.10 ± 0.10	−0.28 ± 0.08
HD 7570	0.13 ± 0.06	0.13 ± 0.08	0.13 ± 0.07	0.13 ± 0.05	0.22 ± 0.11	–	0.19 ± 0.03	0.14 ± 0.04	0.16 ± 0.04
HD 10360	−0.27 ± 0.05	−0.44 ± 0.11	−0.31 ± 0.12	−0.17 ± 0.07	−0.08 ± 0.12	−0.35 ± 0.05	−0.32 ± 0.09	−0.19 ± 0.05	−0.34 ± 0.05
HD 10700	−0.43 ± 0.05	−0.52 ± 0.11	−0.41 ± 0.08	−0.27 ± 0.06	−0.33 ± 0.09	−0.58 ± 0.04	−0.60 ± 0.06	−0.41 ± 0.04	−0.55 ± 0.05
HD 14412	−0.48 ± 0.05	−0.55 ± 0.08	−0.40 ± 0.07	−0.39 ± 0.06	−0.42 ± 0.10	−0.56 ± 0.05	−0.49 ± 0.08	−0.44 ± 0.07	−0.55 ± 0.05
HD 17925	−0.04 ± 0.07	−0.07 ± 0.09	−0.02 ± 0.14	0.09 ± 0.08	0.17 ± 0.12	0.03 ± 0.07	0.01 ± 0.09	0.04 ± 0.07	−0.05 ± 0.07
HD 20010	−0.19 ± 0.09	−0.29 ± 0.16	−0.14 ± 0.19	−0.14 ± 0.36	−0.09 ± 0.21	−0.32 ± 0.11	−0.23 ± 0.10	−0.30 ± 0.17	−0.21 ± 0.09
HD 20766	−0.24 ± 0.03	−0.29 ± 0.07	−0.17 ± 0.10	−0.16 ± 0.04	−0.24 ± 0.10	−0.31 ± 0.06	−0.24 ± 0.09	−0.23 ± 0.10	−0.26 ± 0.03
HD 20794	−0.26 ± 0.05	−0.35 ± 0.10	−0.20 ± 0.09	−0.07 ± 0.07	−0.14 ± 0.09	−0.44 ± 0.05	−0.46 ± 0.05	−0.20 ± 0.05	−0.39 ± 0.03
HD 20807	−0.24 ± 0.03	−0.31 ± 0.06	−0.18 ± 0.09	−0.23 ± 0.05	−0.24 ± 0.03	−0.32 ± 0.04	−0.29 ± 0.09	−0.28 ± 0.08	−0.29 ± 0.03
HD 23249	0.10 ± 0.13	−0.02 ± 0.10	0.10 ± 0.11	0.17 ± 0.10	0.33 ± 0.14	−0.01 ± 0.06	0.23 ± 0.13	0.27 ± 0.08	0.13 ± 0.07
HD 23356	−0.14 ± 0.06	−0.26 ± 0.12	−0.05 ± 0.12	0.02 ± 0.09	0.16 ± 0.14	−0.18 ± 0.05	−0.12 ± 0.12	−0.02 ± 0.07	−0.17 ± 0.06
HD 23484	−0.01 ± 0.04	−0.08 ± 0.11	−0.03 ± 0.12	0.10 ± 0.08	0.19 ± 0.09	0.00 ± 0.05	0.05 ± 0.09	0.07 ±0.07	−0.02 ± 0.05
HD 26965A	−0.20 ± 0.06	−0.39 ± 0.10	−0.18 ± 0.07	−0.01 ± 0.06	−0.02 ± 0.09	−0.36 ± 0.04	−0.40 ± 0.05	−0.10 ± 0.09	−0.31 ± 0.04
HD 30495	−0.06 ± 0.05	−0.07 ± 0.07	−0.04 ± 0.08	0.02 ± 0.07	0.05 ± 0.10	−0.02 ± 0.04	0.00 ± 0.07	−0.01 ± 0.09	−0.06 ± 0.04
HD 36435	−0.10 ± 0.04	−0.15 ± 0.07	−0.04 ± 0.10	−0.01 ± 0.06	0.02 ± 0.08	−0.06 ± 0.04	−0.02 ± 0.06	−0.04 ± 0.07	−0.12 ± 0.02
HD 38858	−0.24 ± 0.05	−0.31 ± 0.08	−0.21 ± 0.10	−0.18 ± 0.05	−0.23 ± 0.06	−0.27 ± 0.06	−0.25 ± 0.07	−0.21 ± 0.10	−0.28 ± 0.05
HD 40307	−0.31 ± 0.09	−0.42 ± 0.15	−0.31 ± 0.17	−0.13 ± 0.11	−0.03 ± 0.13	−0.39 ± 0.06	−0.40 ± 0.05	−0.23 ± 0.10	−0.38 ± 0.06
HD 43162	−0.08 ± 0.04	−0.10 ± 0.07	−0.04 ± 0.11	−0.02 ± 0.05	−0.01 ± 0.06	−0.05 ± 0.06	−0.08 ± 0.06	−0.11 ± 0.06	−0.12 ± 0.06
HD 43834	0.07 ± 0.03	−0.04 ± 0.09	0.10 ± 0.09	0.11 ± 0.06	0.17 ± 0.08	0.03 ± 0.04	0.19 ± 0.09	0.20 ± 0.07	0.09 ± 0.04
HD 50281A	−0.13 ± 0.07	−0.22 ± 0.14	−0.06 ± 0.14	−0.02 ± 0.11	0.26 ± 0.15	−0.14 ± 0.10	−0.14 ± 0.12	−0.02 ± 0.07	−0.17 ± 0.03
HD 52919	−0.13 ± 0.11	−0.07 ± 0.09	−0.15 ± 0.13	0.14 ± 0.10	0.30 ± 0.13	−0.09 ± 0.07	−0.02 ± 0.09	−0.02 ± 0.08	−0.16 ± 0.06
HD 53143	0.17 ± 0.05	0.10 ± 0.09	0.17 ± 0.12	0.22 ± 0.08	0.28 ± 0.11	0.17 ± 0.06	0.23 ± 0.11	0.18 ± 0.06	0.16 ± 0.04
HD 53680	−0.27 ± 0.26	−0.48 ± 0.32	−0.07 ± 0.25	0.07 ± 0.35	0.15 ± 0.38	−0.39 ± 0.20	−0.37 ± 0.19	0.02 ±0.14	−0.34 ± 0.09
HD 53705	−0.18 ± 0.05	−0.24 ± 0.06	−0.11 ± 0.08	−0.12 ± 0.04	−0.15 ± 0.05	−0.31 ± 0.04	−0.29 ± 0.10	−0.14 ± 0.09	−0.24 ± 0.03
HD 53706	−0.24 ± 0.05	−0.32 ± 0.10	−0.22 ± 0.10	−0.08 ± 0.05	−0.09 ± 0.10	−0.32 ± 0.03	−0.26 ± 0.10	−0.13 ± 0.06	−0.29 ± 0.05
HD 57095	−0.04 ± 0.08	−0.10 ± 0.10	0.00 ± 0.17	0.12 ± 0.11	0.20 ± 0.12	−0.03 ± 0.09	−0.05 ± 0.11	−0.01 ± 0.05	−0.10 ± 0.05
HD 59686	0.26 ± 0.35	−0.04 ± 0.15	0.46 ± 0.12	0.28 ± 0.20	0.49 ± 0.23	0.18 ± 0.14	0.58 ± 0.08	0.54 ± 0.13	0.19 ± 0.12
HD 61606	−0.08 ± 0.07	−0.15 ± 0.12	−0.04 ± 0.13	0.11 ± 0.11	0.23 ± 0.15	−0.05 ± 0.09	−0.04 ± 0.07	−0.02 ± 0.09	−0.08 ± 0.07
HD 64606	−0.56 ± 0.09	−0.62 ± 0.11	−0.57 ± 0.11	−0.32 ± 0.12	−0.40 ± 0.12	−0.75 ± 0.07	−0.89 ± 0.11	−0.60 ± 0.08	−0.72 ± 0.06
HD 65277	−0.31 ± 0.08	−0.27 ± 0.14	−0.27 ± 0.14	0.08 ± 0.14	0.28 ± 0.17	−0.21 ± 0.13	−0.25 ± 0.13	−0.14 ± 0.08	−0.30 ± 0.07
HD 65486	−0.31 ± 0.08	−0.52 ± 0.14	−0.30 ± 0.16	−0.20 ± 0.12	−0.13 ± 0.15	−0.42 ± 0.10	−0.30 ± 0.10	−0.30 ± 0.06	−0.42 ± 0.05
HD 65907A	−0.16 ± 0.05	−0.25 ± 0.09	−0.09 ± 0.10	−0.03 ± 0.09	−0.12 ± 0.11	−0.38 ± 0.04	−0.47 ± 0.09	−0.22 ± 0.07	−0.30 ± 0.04
HD 67199	0.03 ± 0.09	−0.13 ± 0.11	−0.11 ± 0.09	0.14 ± 0.09	0.21 ± 0.14	−0.01 ± 0.07	0.05 ± 0.08	0.13 ± 0.10	0.03 ± 0.05
HD 69830	−0.08 ± 0.03	−0.15 ± 0.09	−0.02 ± 0.10	−0.03 ± 0.06	0.08 ± 0.08	−0.10 ± 0.04	−0.04 ± 0.04	0.01 ± 0.08	−0.06 ± 0.03
HD 72673	−0.40 ± 0.04	−0.46 ± 0.10	−0.32 ± 0.11	−0.24 ± 0.05	−0.23 ± 0.06	−0.45 ± 0.04	−0.45 ± 0.09	−0.30 ± 0.06	−0.43 ± 0.03
HD 74576	−0.10 ± 0.06	−0.21 ± 0.11	−0.08 ± 0.12	−0.01 ± 0.09	0.10 ± 0.13	−0.12 ± 0.07	−0.15 ± 0.07	−0.04 ± 0.05	−0.13 ± 0.07
HD 76151	0.08 ± 0.04	0.01 ± 0.07	0.09 ± 0.05	0.12 ± 0.04	0.14 ± 0.09	0.10 ± 0.06	0.18 ± 0.06	0.16 ± 0.06	0.11 ± 0.02
HD 82342	−0.44 ± 0.09	−0.21 ± 0.12	−0.28 ± 0.13	0.18 ± 0.13	0.30 ± 0.15	−0.37 ± 0.10	−0.45 ± 0.13	−0.16 ± 0.08	−0.49 ± 0.08
HD 84117	−0.05 ± 0.05	−0.11 ± 0.07	−0.07 ± 0.09	−0.04 ± 0.08	−0.07 ± 0.12	−0.13 ± 0.06	−0.11 ± 0.08	−0.20 ± 0.13	−0.07 ± 0.07
HD 85512	−0.13 ± 0.23	−0.58 ± 0.33	−0.12 ± 0.32	0.15 ± 0.58	0.33 ± 0.57	−0.30 ± 0.20	−0.32 ± 0.21	0.11 ± 0.17	−0.24 ± 0.14
HD 100623	−0.35 ± 0.06	−0.38 ± 0.12	−0.28 ± 0.10	−0.14 ± 0.07	−0.14 ± 0.12	−0.36 ± 0.08	−0.39 ± 0.09	−0.23 ± 0.05	−0.40 ± 0.06
HD 101581	−0.33 ± 0.12	−0.66 ± 0.17	−0.32 ± 0.14	−0.20 ± 0.20	−0.01 ± 0.20	−0.50 ± 0.13	−0.48 ± 0.16	−0.26 ± 0.06	−0.41 ± 0.10
HD 102365	−0.22 ± 0.07	−0.32 ± 0.08	−0.13 ± 0.08	−0.09 ± 0.06	−0.20 ± 0.08	−0.36 ± 0.06	−0.33 ± 0.05	−0.22 ± 0.06	−0.28 ± 0.06
HD 102438	−0.22 ± 0.06	−0.30 ± 0.09	−0.18 ± 0.09	−0.08 ± 0.07	−0.11 ± 0.13	−0.17 ± 0.06	−0.13 ± 0.07	−0.16 ± 0.06	−0.24 ± 0.06
HD 103166	0.40 ± 0.05	0.19 ± 0.11	0.43 ± 0.10	0.43 ± 0.10	0.56 ± 0.12	0.26 ± 0.07	0.50 ± 0.15	0.48 ± 0.09	0.45 ± 0.07
HD 103932	0.05 ± 0.09	−0.01 ± 0.17	0.14 ± 0.17	0.38 ± 0.19	0.61 ± 0.21	0.08 ± 0.13	0.25 ± 0.11	0.26 ± 0.12	0.05 ± 0.10
HD 104304	0.29 ± 0.05	0.13 ± 0.07	0.35 ± 0.08	0.29 ± 0.07	0.36 ± 0.08	0.21 ± 0.05	0.42 ± 0.15	0.43 ± 0.09	0.33 ± 0.06
HD 109200	−0.24 ± 0.08	−0.36 ± 0.09	−0.21 ± 0.10	−0.10 ± 0.07	−0.08 ± 0.11	−0.32 ± 0.05	−0.35 ± 0.04	−0.21 ± 0.07	−0.32 ± 0.06
HD 111261	−0.53 ± 0.13	−0.53 ± 0.13	−0.38 ± 0.16	−0.14 ± 0.14	−0.07 ± 0.17	−0.41 ± 0.11	−0.52 ± 0.16	−0.28 ± 0.05	−0.48 ± 0.11
HD 114386	−0.05 ± 0.09	−0.11 ± 0.14	−0.04 ± 0.15	0.14 ± 0.14	0.37 ± 0.17	−0.04 ± 0.09	−0.02 ± 0.09	0.05 ± 0.10	−0.10 ± 0.05
HD 115617	−0.01 ± 0.05	−0.09 ± 0.07	0.14 ± 0.08	0.08 ± 0.07	0.05 ± 0.09	−0.02 ± 0.05	0.04 ± 0.06	0.02 ± 0.06	−0.03 ± 0.04
HD 118972	−0.06 ± 0.06	−0.10 ± 0.09	−0.04 ± 0.11	0.05 ± 0.10	0.11 ± 0.11	−0.04 ± 0.07	−0.03 ± 0.07	−0.07 ± 0.07	−0.12 ± 0.05
HD 125072	0.27 ± 0.11	0.12 ± 0.16	0.32 ± 0.14	0.39 ± 0.17	0.68 ± 0.19	0.20 ± 0.11	0.42 ± 0.11	0.45 ± 0.11	0.24 ± 0.09
HD 128620	0.27 ± 0.04	0.17 ± 0.07	0.37 ± 0.10	0.28 ± 0.06	0.37 ± 0.06	0.21 ± 0.04	0.34 ± 0.09	0.38 ± 0.04	0.31 ± 0.05
HD 128621	0.23 ± 0.06	0.00 ± 0.12	0.26 ± 0.11	0.26 ± 0.12	0.44 ± 0.14	0.13 ± 0.08	0.30 ± 0.17	0.40 ± 0.10	0.24 ± 0.06

Table 8. continued.

Star (HD)	[Si/H]	[Ca/H]	[Sc/H]	[Ti/H]	[V/H]	[Cr/H]	[Mn/H]	[Co/H]	[Ni/H]
HD 130922	−0.08 ± 0.09	−0.21 ± 0.14	−0.06 ± 0.15	0.04 ± 0.14	0.24 ± 0.17	−0.13 ± 0.10	−0.09 ± 0.13	0.03 ± 0.08	−0.11 ± 0.09
HD 131977	0.00 ± 0.08	−0.11 ± 0.14	0.15 ± 0.16	0.17 ± 0.14	0.39 ± 0.17	−0.04 ± 0.09	0.06 ± 0.13	0.16 ± 0.09	0.01 ± 0.07
HD 135204	−0.05 ± 0.05	−0.16 ± 0.09	0.09 ± 0.12	0.08 ± 0.05	0.01 ± 0.08	−0.18 ± 0.04	−0.11 ± 0.10	0.03 ± 0.07	−0.11 ± 0.04
HD 136352	−0.20 ± 0.06	−0.30 ± 0.07	−0.10 ± 0.13	−0.11 ± 0.07	−0.21 ± 0.12	−0.38 ± 0.06	−0.44 ± 0.09	−0.22 ± 0.08	−0.30 ± 0.04
HD 140901	0.08 ± 0.04	0.03 ± 0.10	0.14 ± 0.07	0.17 ± 0.06	0.24 ± 0.09	0.07 ± 0.07	0.22 ± 0.07	0.15 ± 0.06	0.12 ± 0.04
HD 142709	−0.27 ± 0.11	−0.25 ± 0.15	−0.09 ± 0.17	0.31 ± 0.17	0.55 ± 0.20	−0.17 ± 0.14	−0.29 ± 0.10	−0.05 ± 0.12	−0.36 ± 0.07
HD 144628	−0.33 ± 0.08	−0.40 ± 0.11	−0.31 ± 0.08	−0.13 ± 0.07	−0.12 ± 0.12	−0.41 ± 0.06	−0.45 ± 0.04	−0.27 ± 0.05	−0.33 ± 0.06
HD 145417	−1.16 ± 0.09	−0.97 ± 0.17	−1.07 ± 0.15	−0.66 ± 0.17	−0.82 ± 0.18	−1.19 ± 0.12	−1.36 ± 0.10	−1.15 ± 0.12	−1.28 ± 0.07
HD 146233	0.06 ± 0.05	−0.01 ± 0.06	0.05 ± 0.08	0.06 ± 0.05	0.07 ± 0.06	−0.01 ± 0.07	0.08 ± 0.07	0.05 ± 0.08	0.02 ± 0.03
HD 149661	0.02 ± 0.05	−0.06 ± 0.08	0.03 ± 0.11	0.11 ± 0.07	0.18 ± 0.10	0.00 ± 0.06	0.05 ± 0.08	0.11 ± 0.07	−0.01 ± 0.05
HD 150689	−0.13 ± 0.09	−0.13 ± 0.13	−0.16 ± 0.16	0.10 ± 0.15	0.25 ± 0.17	−0.07 ± 0.10	−0.12 ± 0.10	−0.05 ± 0.07	−0.17 ± 0.07
HD 152391	−0.03 ± 0.07	−0.06 ± 0.06	0.01 ± 0.08	0.10 ± 0.06	0.11 ± 0.10	0.00 ± 0.06	0.00 ± 0.06	−0.01 ± 0.06	−0.06 ± 0.05
HD 154088	0.33 ± 0.06	0.18 ± 0.10	0.34 ± 0.10	0.41 ± 0.09	0.50 ± 0.10	0.24 ± 0.07	0.48 ± 0.16	0.45 ± 0.09	0.35 ± 0.07
HD 154363	−0.27 ± 0.16	−0.78 ± 0.22	−0.36 ± 0.19	−0.18 ± 0.27	−0.06 ± 0.28	−0.60 ± 0.20	−0.83 ± 0.18	−0.32 ± 0.10	−0.55 ± 0.12
HD 154577	−0.61 ± 0.10	−0.73 ± 0.12	−0.49 ± 0.11	−0.37 ± 0.11	−0.34 ± 0.10	−0.63 ± 0.08	−0.73 ± 0.05	0.52 ± 0.07	−0.65 ± 0.06
HD 156026	−0.31 ± 0.14	−0.57 ± 0.18	−0.19 ± 0.17	−0.07 ± 0.18	0.09 ± 0.20	−0.36 ± 0.13	−0.47 ± 0.14	−0.13 ± 0.08	−0.28 ± 0.09
HD 156274	−0.27 ± 0.07	−0.35 ± 0.09	−0.28 ± 0.10	−0.12 ± 0.05	−0.13 ± 0.09	−0.35 ± 0.06	−0.37 ± 0.06	−0.25 ± 0.04	−0.37 ± 0.04
HD 156384	−0.59 ± 0.16	−0.41 ± 0.20	−0.41 ± 0.18	−0.04 ± 0.17	0.10 ± 0.20	−0.46 ± 0.14	−0.56 ± 0.11	−0.37 ± 0.08	−0.61 ± 0.09
HD 165185	−0.05 ± 0.06	−0.07 ± 0.09	−0.04 ± 0.09	0.01 ± 0.13	0.05 ± 0.10	−0.10 ± 0.07	−0.04 ± 0.10	−0.10 ± 0.10	−0.09 ± 0.09
HD 165499	−0.02 ± 0.04	−0.08 ± 0.05	0.03 ± 0.07	0.00 ± 0.05	−0.05 ± 0.08	−0.10 ± 0.06	−0.12 ± 0.09	−0.03 ± 0.07	−0.04 ± 0.06
HD 170493	0.12 ± 0.10	0.01 ± 0.15	0.16 ± 0.15	0.39 ± 0.21	0.47 ± 0.19	0.19 ± 0.16	0.37 ± 0.08	0.35 ± 0.12	0.13 ± 0.05
HD 170573	−0.18 ± 0.11	−0.22 ± 0.17	−0.10 ± 0.21	0.21 ± 0.17	0.41 ± 0.17	−0.02 ± 0.12	−0.08 ± 0.16	0.06 ± 0.08	−0.19 ± 0.07
HD 170657	−0.21 ± 0.07	−0.28 ± 0.11	−0.21 ± 0.11	−0.05 ± 0.09	0.01 ± 0.10	−0.21 ± 0.08	−0.24 ± 0.09	−0.12 ± 0.05	−0.26 ± 0.05
HD 172051	−0.22 ± 0.07	−0.26 ± 0.08	−0.23 ± 0.11	−0.09 ± 0.07	−0.10 ± 0.08	−0.26 ± 0.04	−0.27 ± 0.06	−0.19 ± 0.06	−0.25 ± 0.04
HD 177565	0.14 ± 0.03	0.03 ± 0.08	0.17 ± 0.08	0.18 ± 0.05	0.23 ± 0.08	0.06 ± 0.06	0.22 ± 0.09	0.17 ± 0.05	0.16 ± 0.04
HD 191408A	−0.49 ± 0.06	−0.45 ± 0.14	−0.49 ± 0.13	−0.10 ± 0.09	−0.13 ± 0.10	−0.53 ± 0.06	−0.60 ± 0.08	−0.36 ± 0.05	−0.59 ± 0.05
HD 192310	0.01 ± 0.08	−0.18 ± 0.14	−0.02 ± 0.09	0.18 ± 0.14	0.25 ± 0.15	−0.05 ± 0.05	0.11 ± 0.06	0.17 ± 0.11	0.01 ± 0.06
HD 196761	−0.30 ± 0.05	−0.39 ± 0.07	−0.27 ± 0.11	−0.22 ± 0.07	−0.21 ± 0.09	−0.33 ± 0.05	−0.29 ± 0.07	−0.23 ± 0.03	−0.34 ± 0.03
HD 207129	−0.05 ± 0.04	−0.07 ± 0.07	0.03 ± 0.09	−0.02 ± 0.07	−0.01 ± 0.05	−0.11 ± 0.06	−0.06 ± 0.09	−0.08 ± 0.09	−0.07 ± 0.03
HD 209100	−0.14 ± 0.09	−0.33 ± 0.15	−0.07 ± 0.14	−0.06 ± 0.16	0.07 ± 0.19	−0.22 ± 0.10	−0.21 ± 0.10	0.04 ± 0.11	−0.19 ± 0.09
HD 211415	−0.22 ± 0.05	−0.28 ± 0.06	−0.12 ± 0.08	−0.15 ± 0.04	−0.18 ± 0.09	−0.28 ± 0.07	−0.25 ± 0.08	−0.22 ± 0.10	−0.23 ± 0.03
HD 216803	−0.10 ± 0.11	−0.41 ± 0.14	0.03 ± 0.11	−0.13 ± 0.17	0.18 ± 0.20	−0.23 ± 0.12	−0.13 ± 0.12	0.00 ± 0.07	−0.16 ± 0.07
HD 222237	−0.33 ± 0.05	−0.46 ± 0.14	−0.21 ± 0.12	−0.02 ± 0.14	0.34 ± 0.17	−0.43 ± 0.08	−0.09 ± 0.09	−0.04 ± 0.07	−0.38 ± 0.07
HD 222335	−0.21 ± 0.06	−0.27 ± 0.09	−0.30 ± 0.12	−0.08 ± 0.08	−0.02 ± 0.10	−0.20 ± 0.06	−0.18 ± 0.05	−0.11 ± 0.07	−0.26 ± 0.05

Table 9. Abundances of Na, Mg and Al (from Beirão et al. 2005, with the addition of our results) and atmospheric parameters (from Santos et al. 2004b, 2005) for stars with planets.

Star (HD)	[Na/H]	[Mg/H]	[Al/H]	$T_{\rm eff}$ [K]	$\log g$ [cm s^{-2}]	$\xi_{\rm t}$ [km s^{-1}]	[Fe/H]
HD 142	0.28 ± 0.07	0.16 ± 0.06	–	6302 ± 56	4.34 ± 0.13	1.86 ± 0.17	0.14 ± 0.07
HD 1237	−0.08 ± 0.07	0.04 ± 0.04	0.03 ± 0.07	5536 ± 50	4.56 ± 0.12	1.33 ± 0.06	0.12 ± 0.06
HD 2039	0.38 ± 0.06	0.35 ± 0.04	0.42 ± 0.03	5976 ± 51	4.45 ± 0.10	1.26 ± 0.07	0.32 ± 0.06
HD 3651	0.00 ± 0.04	0.17 ± 0.05	0.24 ± 0.04	5173 ± 35	4.37 ± 0.12	0.74 ± 0.05	0.12 ± 0.04
HD 4203	0.42 ± 0.05	0.48 ± 0.06	0.51 ± 0.03	5636 ± 40	4.23 ± 0.14	1.12 ± 0.05	0.40 ± 0.05
HD 4208	−0.22 ± 0.04	−0.12 ± 0.08	−0.10 ± 0.02	5626 ± 32	4.49 ± 0.10	0.95 ± 0.06	−0.24 ± 0.04
HD 6434	−0.38 ± 0.07	−0.21 ± 0.07	−0.24 ± 0.07	5835 ± 59	4.60 ± 0.12	1.53 ± 0.27	−0.52 ± 0.08
HD 8574	0.04 ± 0.04	0.12 ± 0.07	0.04 ± 0.07	6151 ± 57	4.51 ± 0.10	1.45 ± 0.15	0.06 ± 0.07
HD 9826	0.25 ± 0.05	0.24 ± 0.07	–	6212 ± 64	4.26 ± 0.13	1.69 ± 0.16	0.13 ± 0.08
HD 10647	−0.06 ± 0.06	0.02 ± 0.06	−0.07 ± 0.04	6143 ± 31	4.48 ± 0.08	1.40 ± 0.08	−0.03 ± 0.04
HD 10697	0.14 ± 0.03	0.17 ± 0.06	0.21 ± 0.03	5641 ± 28	4.05 ± 0.05	1.13 ± 0.03	0.14 ± 0.04
HD 12661	0.41 ± 0.07	0.47 ± 0.04	0.43 ± 0.03	5702 ± 36	4.33 ± 0.08	1.05 ± 0.04	0.36 ± 0.05
HD 13445	−0.29 ± 0.07	−0.03 ± 0.04	−0.04 ± 0.03	5163 ± 36	4.52 ± 0.12	0.72 ± 0.06	−0.24 ± 0.04
HD 16141	0.11 ± 0.05	0.17 ± 0.03	0.21 ± 0.04	5801 ± 30	4.22 ± 0.12	1.34 ± 0.04	0.15 ± 0.04
HD 17051	0.24 ± 0.03	0.19 ± 0.06	0.19 ± 0.03	6252 ± 53	4.61 ± 0.16	1.18 ± 0.10	0.26 ± 0.06
HD 19994	0.48 ± 0.05	0.21 ± 0.04	0.32 ± 0.03	6190 ± 56	4.19 ± 0.12	1.54 ± 0.06	0.24 ± 0.07
HD 20367	0.10 ± 0.05	0.19 ± 0.08	0.17 ± 0.05	6138 ± 79	4.53 ± 0.22	1.22 ± 0.16	0.17 ± 0.10
HD 22049	−0.23 ± 0.05	−0.04 ± 0.04	−0.07 ± 0.03	5073 ± 42	4.43 ± 0.08	1.05 ± 0.06	−0.13 ± 0.04
HD 23079	−0.08 ± 0.05	−0.04 ± 0.06	−0.06 ± 0.03	5959 ± 46	4.35 ± 0.12	1.20 ± 0.10	−0.11 ± 0.06
HD 23596	0.47 ± 0.06	0.33 ± 0.06	0.32 ± 0.05	6108 ± 36	4.25 ± 0.10	1.30 ± 0.05	0.31 ± 0.05
HD 27442	0.41 ± 0.25	0.51 ± 0.07	0.53 ± 0.08	4825 ± 107	3.55 ± 0.32	1.18 ± 0.12	0.39 ± 0.13
HD 28185	0.27 ± 0.05	0.18 ± 0.05	0.30 ± 0.03	5656 ± 44	4.45 ± 0.08	1.01 ± 0.06	0.22 ± 0.05
HD 30177	0.44 ± 0.06	0.46 ± 0.06	0.54 ± 0.05	5588 ± 57	4.29 ± 0.12	1.08 ± 0.06	0.39 ± 0.07
HD 33636	−0.10 ± 0.05	−0.07 ± 0.04	−0.02 ± 0.03	6046 ± 49	4.71 ± 0.09	1.79 ± 0.19	−0.08 ± 0.06
HD 37124	−0.32 ± 0.05	−0.13 ± 0.02	−0.11 ± 0.03	5546 ± 30	4.50 ± 0.03	0.80 ± 0.07	−0.38 ± 0.04
HD 38529	0.48 ± 0.06	0.47 ± 0.03	0.47 ± 0.04	5674 ± 40	3.94 ± 0.12	1.38 ± 0.05	0.40 ± 0.06
HD 39091	0.17 ± 0.04	0.15 ± 0.04	0.17 ± 0.03	5991 ± 27	4.42 ± 0.10	1.24 ± 0.04	0.10 ± 0.04
HD 40979	0.34 ± 0.04	0.33 ± 0.05	–	6145 ± 42	4.31 ± 0.15	1.29 ± 0.09	0.21 ± 0.05
HD 46375	0.19 ± 0.06	0.39 ± 0.04	0.32 ± 0.06	5268 ± 55	4.41 ± 0.16	0.97 ± 0.06	0.20 ± 0.06
HD 47536	−0.42 ± 0.31	−0.25 ± 0.06	−0.20 ± 0.10	4554 ± 85	2.48 ± 0.23	1.82 ± 0.08	−0.54 ± 0.12
HD 49674	0.22 ± 0.05	0.35 ± 0.06	–	5644 ± 54	4.37 ± 0.07	0.89 ± 0.07	0.33 ± 0.06
HD 50554	0.03 ± 0.06	0.04 ± 0.03	0.00 ± 0.02	6026 ± 30	4.41 ± 0.13	1.11 ± 0.06	0.01 ± 0.04
HD 52265	0.24 ± 0.06	0.20 ± 0.05	0.24 ± 0.03	6103 ± 52	4.28 ± 0.15	1.36 ± 0.08	0.23 ± 0.06
HD 65216	−0.20 ± 0.02	−0.12 ± 0.04	−0.09 ± 0.05	5666 ± 31	4.53 ± 0.09	1.06 ± 0.05	−0.12 ± 0.04
HD 68988	0.40 ± 0.04	0.39 ± 0.04	0.39 ± 0.05	5988 ± 52	4.45 ± 0.15	1.25 ± 0.08	0.36 ± 0.06
HD 70642	0.23 ± 0.06	0.36 ± 0.04	0.28 ± 0.03	5693 ± 26	4.41 ± 0.09	1.01 ± 0.04	0.18 ± 0.04
HD 72659	0.07 ± 0.04	0.11 ± 0.06	0.07 ± 0.06	5995 ± 45	4.30 ± 0.07	1.42 ± 0.09	0.03 ± 0.06
HD 73256	0.30 ± 0.06	0.37 ± 0.04	0.33 ± 0.06	5518 ± 49	4.42 ± 0.12	1.22 ± 0.06	0.26 ± 0.06
HD 73526	0.24 ± 0.04	0.40 ± 0.05	0.38 ± 0.06	5699 ± 49	4.27 ± 0.12	1.26 ± 0.06	0.27 ± 0.06
HD 74156	0.21 ± 0.03	0.18 ± 0.03	0.27 ± 0.02	6112 ± 39	4.34 ± 0.10	1.38 ± 0.07	0.16 ± 0.05
HD 75289	0.13 ± 0.04	0.24 ± 0.04	0.26 ± 0.03	6143 ± 53	4.42 ± 0.13	1.53 ± 0.09	0.28 ± 0.07
HD 75732	0.26 ± 0.07	0.48 ± 0.06	0.47 ± 0.04	5279 ± 62	4.37 ± 0.18	0.98 ± 0.07	0.33 ± 0.07
HD 76700	0.40 ± 0.06	0.54 ± 0.05	0.52 ± 0.04	5737 ± 34	4.25 ± 0.14	1.18 ± 0.04	0.41 ± 0.05
HD 80606	0.30 ± 0.08	0.41 ± 0.06	0.49 ± 0.06	5574 ± 72	4.46 ± 0.20	1.14 ± 0.09	0.32 ± 0.09
HD 82943	0.29 ± 0.02	0.22 ± 0.04	0.25 ± 0.04	6016 ± 30	4.46 ± 0.07	1.13 ± 0.04	0.30 ± 0.03
HD 83443	0.44 ± 0.06	0.36 ± 0.05	0.70 ± 0.10	5501 ± 63	4.46 ± 0.09	1.07 ± 0.08	0.39 ± 0.07
HD 89744	0.45 ± 0.04	–	0.36 ± 0.06	6234 ± 45	3.98 ± 0.05	1.62 ± 0.08	0.22 ± 0.05
HD 92788	0.38 ± 0.06	0.35 ± 0.02	0.43 ± 0.03	5758 ± 37	4.3 ± 0.04	1.1 ± 0.04	0.33 ± 0.05
HD 95128	0.07 ± 0.03	0.09 ± 0.04	0.09 ± 0.03	5954 ± 25	4.44 ± 0.10	1.30 ± 0.04	0.06 ± 0.03
HD 104985	−0.18 ± 0.21	−0.10 ± 0.03	−0.01 ± 0.05	4773 ± 62	2.76 ± 0.14	1.71 ± 0.07	−0.28 ± 0.09
HD 106252	0.01 ± 0.03	0.06 ± 0.05	0.01 ± 0.02	5899 ± 35	4.34 ± 0.07	1.08 ± 0.06	−0.01 ± 0.05
HD 108147	0.18 ± 0.06	0.21 ± 0.04	–	6248 ± 42	4.49 ± 0.16	1.35 ± 0.08	0.20 ± 0.05
HD 108874	0.13 ± 0.07	0.27 ± 0.03	0.30 ± 0.04	5596 ± 42	4.37 ± 0.12	0.89 ± 0.05	0.23 ± 0.05
HD 111232	−0.33 ± 0.05	−0.11 ± 0.03	−0.1 ± 0.04	5494 ± 26	4.50 ± 0.10	0.84 ± 0.05	−0.36 ± 0.04
HD 114386	–	0.07 ± 0.07	0.12 ± 0.05	4804 ± 61	4.36 ± 0.28	0.57 ± 0.12	−0.08 ± 0.06
HD 114729	−0.26 ± 0.06	−0.09 ± 0.05	−0.13 ± 0.06	5886 ± 36	4.28 ± 0.13	1.25 ± 0.09	−0.25 ± 0.05
HD 114762	−0.59 ± 0.03	−0.40 ± 0.02	−0.56 ± 0.03	5884 ± 34	4.22 ± 0.02	1.31 ± 0.17	−0.70 ± 0.04
HD 114783	−0.11 ± 0.04	0.16 ± 0.04	0.18 ± 0.06	5098 ± 36	4.45 ± 0.11	0.74 ± 0.05	0.09 ± 0.04
HD 117176	−0.10 ± 0.04	0.04 ± 0.03	0.12 ± 0.06	5560 ± 34	4.07 ± 0.05	1.18 ± 0.05	−0.06 ± 0.05
HD 120136	0.44 ± 0.05	–	–	6339 ± 73	4.19 ± 0.10	1.70 ± 0.16	0.23 ± 0.07
HD 121504	0.10 ± 0.03	0.10 ± 0.06	0.19 ± 0.06	6075 ± 40	4.64 ± 0.12	1.31 ± 0.07	0.16 ± 0.05
HD 128311	−0.26 ± 0.08	0.09 ± 0.06	0.07 ± 0.06	4835 ± 72	4.44 ± 0.21	0.89 ± 0.11	0.03 ± 0.07
HD 130322	−0.17 ± 0.07	0.05 ± 0.06	0.07 ± 0.02	5392 ± 36	4.48 ± 0.06	0.85 ± 0.05	0.03 ± 0.04
HD 134987	0.30 ± 0.05	0.39 ± 0.04	0.38 ± 0.03	5776 ± 29	4.36 ± 0.07	1.09 ± 0.04	0.30 ± 0.04
HD 136118	0.02 ± 0.04	0.14 ± 0.04	–	6222 ± 39	4.27 ± 0.15	1.79 ± 0.12	−0.04 ± 0.05
HD 137759	0.17 ± 0.40	0.08 ± 0.08	0.21 ± 0.09	4775 ± 113	3.09 ± 0.40	1.78 ± 0.11	0.13 ± 0.14
HD 141937	0.05 ± 0.03	0.21 ± 0.05	0.13 ± 0.04	5909 ± 39	4.51 ± 0.08	1.13 ± 0.06	0.10 ± 0.05
HD 142415	0.15 ± 0.04	0.17 ± 0.04	0.17 ± 0.04	6045 ± 44	4.53 ± 0.08	1.12 ± 0.07	0.21 ± 0.05
HD 143761	−0.18 ± 0.03	−0.07 ± 0.03	−0.04 ± 0.05	5853 ± 25	4.41 ± 0.15	1.35 ± 0.07	−0.21 ± 0.04
HD 145675	0.40 ± 0.08	0.50 ± 0.05	0.52 ± 0.06	5311 ± 87	4.42 ± 0.18	0.92 ± 0.10	0.43 ± 0.08
HD 147513	−0.08 ± 0.03	0.09 ± 0.04	0.06 ± 0.02	5894 ± 31	4.43 ± 0.02	1.26 ± 0.05	0.08 ± 0.04
HD 150706	−0.08 ± 0.04	0.01 ± 0.06	−0.12 ± 0.03	5961 ± 27	4.50 ± 0.10	1.11 ± 0.06	−0.01 ± 0.04
HD 160691	0.38 ± 0.05	0.35 ± 0.04	0.39 ± 0.03	5798 ± 33	4.31 ± 0.08	1.19 ± 0.04	0.32 ± 0.04
HD 162020	−0.28 ± 0.10	0.06 ± 0.06	0.05 ± 0.06	4858 ± 81	4.42 ± 0.30	0.86 ± 0.14	−0.04 ± 0.07
HD 168443	0.04 ± 0.03	0.17 ± 0.03	0.24 ± 0.03	5617 ± 35	4.22 ± 0.05	1.21 ± 0.05	0.06 ± 0.05
HD 168746	−0.04 ± 0.05	0.18 ± 0.03	0.23 ± 0.05	5601 ± 33	4.41 ± 0.12	0.99 ± 0.05	−0.08 ± 0.05
HD 169830	0.41 ± 0.02	0.18 ± 0.06	0.18 ± 0.03	6299 ± 41	4.10 ± 0.02	1.42 ± 0.09	0.21 ± 0.05
HD 177830	0.37 ± 0.14	0.56 ± 0.06	0.54 ± 0.07	4804 ± 77	3.57 ± 0.17	1.14 ± 0.09	0.33 ± 0.09
HD 178911	0.12 ± 0.07	0.30 ± 0.04	0.27 ± 0.03	5600 ± 42	4.44 ± 0.08	0.95 ± 0.05	0.27 ± 0.05

Table 9. continued.

Star (HD)	[Na/H]	[Mg/H]	[Al/H]	$T_{\rm eff}$ [K]	$\log g$ [cm s^{-2}]	$\xi_{\rm t}$ [km s^{-1}]	[Fe/H]
HD 179949	0.30 ± 0.02	0.22 ± 0.06	–	6260 ± 43	4.43 ± 0.05	1.41 ± 0.09	0.22 ± 0.05
HD 186427	0.07 ± 0.02	0.12 ± 0.05	0.11 ± 0.03	5772 ± 25	4.40 ± 0.07	1.07 ± 0.04	0.08 ± 0.04
HD 187123	0.15 ± 0.02	0.14 ± 0.02	0.13 ± 0.02	5845 ± 22	4.42 ± 0.07	1.10 ± 0.03	0.13 ± 0.03
HD 190228	−0.24 ± 0.04	−0.16 ± 0.03	−0.12 ± 0.02	5327 ± 34	3.90 ± 0.07	1.11 ± 0.04	−0.26 ± 0.05
HD 190360	0.26 ± 0.05	0.33 ± 0.04	0.34 ± 0.05	5584 ± 36	4.37 ± 0.06	1.07 ± 0.05	0.24 ± 0.05
HD 192263	–	0.07 ± 0.06	0.02 ± 0.04	4947 ± 58	4.51 ± 0.20	0.86 ± 0.09	−0.02 ± 0.06
HD 195019A	0.04 ± 0.03	0.13 ± 0.03	0.19 ± 0.02	5842 ± 35	4.32 ± 0.07	1.27 ± 0.05	0.08 ± 0.04
HD 196050	0.34 ± 0.04	0.31 ± 0.05	0.40 ± 0.03	5918 ± 44	4.35 ± 0.13	1.39 ± 0.06	0.22 ± 0.05
HD 202206	0.38 ± 0.04	0.41 ± 0.07	0.37 ± 0.03	5752 ± 53	4.50 ± 0.09	1.01 ± 0.06	0.35 ± 0.06
HD 209458	−0.04 ± 0.02	0.01 ± 0.03	0.00 ± 0.02	6117 ± 26	4.48 ± 0.08	1.40 ± 0.06	0.02 ± 0.03
HD 210277	0.2 ± 0.05	0.32 ± 0.06	0.35 ± 0.03	5532 ± 27	4.29 ± 0.13	1.04 ± 0.03	0.19 ± 0.04
HD 213240	0.22 ± 0.05	0.23 ± 0.04	0.20 ± 0.02	5984 ± 33	4.25 ± 0.10	1.25 ± 0.05	0.17 ± 0.05
HD 216435	0.37 ± 0.03	0.31 ± 0.05	0.32 ± 0.02	5938 ± 42	4.12 ± 0.05	1.28 ± 0.06	0.24 ± 0.05
HD 216437	0.35 ± 0.06	0.31 ± 0.03	0.40 ± 0.03	5887 ± 32	4.30 ± 0.07	1.31 ± 0.04	0.25 ± 0.04
HD 216770	0.18 ± 0.04	0.43 ± 0.02	0.37 ± 0.06	5423 ± 41	4.40 ± 0.13	1.01 ± 0.05	0.26 ± 0.04
HD 217014	0.25 ± 0.05	0.3 ± 0.04	0.31 ± 0.02	5804 ± 36	4.42 ± 0.07	1.20 ± 0.05	0.20 ± 0.05
HD 217107	0.38 ± 0.05	0.41 ± 0.05	0.44 ± 0.03	5646 ± 34	4.31 ± 0.10	1.06 ± 0.04	0.37 ± 0.05
HD 219449	−0.09 ± 0.31	0.04 ± 0.09	0.25 ± 0.11	4757 ± 102	2.71 ± 0.25	1.71 ± 0.09	0.05 ± 0.13
HD 219542	0.02 ± 0.02	0.14 ± 0.12	0.16 ± 0.13	5732 ± 31	4.40 ± 0.05	0.99 ± 0.04	0.17 ± 0.04
HD 222404	0.12 ± 0.18	0.34 ± 0.05	0.40 ± 0.07	4916 ± 70	3.36 ± 0.21	1.27 ± 0.06	0.16 ± 0.08
HD 222582	0.05 ± 0.03	0.16 ± 0.03	0.15 ± 0.04	5843 ± 38	4.45 ± 0.07	1.03 ± 0.06	0.05 ± 0.05
HD 330075	−0.05 ± 0.06	0.17 ± 0.02	0.35 ± 0.04	5017 ± 53	4.22 ± 0.11	0.69 ± 0.08	0.08 ± 0.06

Table 10. Abundances of Na, Mg and Al (from Beirão et al. 2005, with the addition of our results) and atmospheric parameters (from Santos et al. 2004b, 2005) for stars without planets.

Star (HD)	[Na/H]	[Mg/H]	[Al/H]	$T_{\rm eff}$ [K]	$\log g$ [cm s^{-2}]	$\xi_{\rm t}$ [km s^{-1}]	[Fe/H]
HD 1581	−0.10 ± 0.06	−0.02 ± 0.02	−0.14 ± 0.03	5956 ± 44	4.39 ± 0.13	1.07 ± 0.09	−0.14 ± 0.05
HD 4391	−0.09 ± 0.06	0.10 ± 0.03	−0.02 ± 0.03	5878 ± 53	4.74 ± 0.15	1.13 ± 0.10	−0.03 ± 0.06
HD 5133	−0.27 ± 0.07	−0.03 ± 0.05	−0.07 ± 0.04	4911 ± 54	4.49 ± 0.18	0.71 ± 0.11	−0.17 ± 0.06
HD 7570	0.24 ± 0.05	0.22 ± 0.03	0.20 ± 0.03	6140 ± 41	4.39 ± 0.16	1.50 ± 0.08	0.18 ± 0.05
HD 10360	−0.29 ± 0.06	−0.13 ± 0.04	−0.13 ± 0.03	4970 ± 40	4.49 ± 0.10	0.76 ± 0.07	−0.26 ± 0.04
HD 10700	−0.52 ± 0.04	−0.23 ± 0.02	−0.24 ± 0.03	5344 ± 29	4.57 ± 0.09	0.91 ± 0.06	−0.52 ± 0.04
HD 14412	−0.42 ± 0.04	−0.3 ± 0.03	−0.34 ± 0.03	5368 ± 24	4.55 ± 0.05	0.88 ± 0.05	−0.47 ± 0.03
HD 17925	−0.03 ± 0.07	0.20 ± 0.05	0.08 ± 0.04	5180 ± 56	4.44 ± 0.13	1.33 ± 0.08	0.06 ± 0.07
HD 20010	−0.10 ± 0.08	−0.13 ± 0.12	–	6275 ± 57	4.40 ± 0.37	2.41 ± 0.41	−0.19 ± 0.06
HD 20766	−0.23 ± 0.02	−0.02 ± 0.02	−0.08 ± 0.03	5733 ± 31	4.55 ± 0.10	1.09 ± 0.06	−0.21 ± 0.04
HD 20794	−0.28 ± 0.05	−0.05 ± 0.03	−0.03 ± 0.03	5444 ± 31	4.47 ± 0.07	0.98 ± 0.06	−0.38 ± 0.04
HD 20807	−0.24 ± 0.03	−0.11 ± 0.05	−0.18 ± 0.03	5843 ± 26	4.47 ± 0.10	1.17 ± 0.06	−0.23 ± 0.04
HD 23249	0.12 ± 0.11	0.22 ± 0.05	0.25 ± 0.05	5074 ± 60	3.77 ± 0.16	1.08 ± 0.06	0.13 ± 0.08
HD 23356	−0.26 ± 0.05	0.00 ± 0.05	0.00 ± 0.04	4975 ± 55	4.48 ± 0.16	0.77 ± 0.09	−0.11 ± 0.06
HD 23484	−0.06 ± 0.08	0.12 ± 0.05	0.09 ± 0.04	5176 ± 45	4.41 ± 0.17	1.03 ± 0.06	0.06 ± 0.05
HD 26965	−0.26 ± 0.03	−0.02 ± 0.03	0.00 ± 0.03	5126 ± 34	4.51 ± 0.08	0.60 ± 0.07	−0.31 ± 0.04
HD 30495	−0.05 ± 0.04	0.05 ± 0.03	0.05 ± 0.02	5868 ± 30	4.55 ± 0.10	1.24 ± 0.05	0.02 ± 0.04
HD 36435	−0.12 ± 0.06	0.04 ± 0.02	−0.03 ± 0.03	5479 ± 37	4.61 ± 0.07	1.12 ± 0.05	−0.00 ± 0.05
HD 38858	−0.22 ± 0.02	−0.13 ± 0.04	−0.13 ± 0.02	5752 ± 32	4.53 ± 0.07	1.26 ± 0.07	−0.23 ± 0.05
HD 40307	–	−0.15 ± 0.08	−0.14 ± 0.07	4805 ± 52	4.37 ± 0.37	0.49 ± 0.12	−0.30 ± 0.05
HD 43162	−0.08 ± 0.05	0.09 ± 0.01	0.02 ± 0.03	5633 ± 35	4.48 ± 0.07	1.24 ± 0.05	−0.01 ± 0.04
HD 43834	0.09 ± 0.04	0.25 ± 0.03	0.24 ± 0.05	5594 ± 36	4.41 ± 0.09	1.05 ± 0.04	0.10 ± 0.05
HD 50281A	−0.36 ± 0.09	0.04 ± 0.07	0.00 ± 0.05	4658 ± 56	4.32 ± 0.24	0.64 ± 0.15	−0.04 ± 0.07
HD 52919	−0.06 ± 0.13	−0.07 ± 0.13	0.11 ± 0.07	4740 ± 49	4.25 ± 0.1	1.03 ± 0.09	−0.05 ± 0.06
HD 53143	0.16 ± 0.08	0.16 ± 0.05	0.29 ± 0.04	5462 ± 54	4.47 ± 0.07	1.08 ± 0.07	0.22 ± 0.06
HD 53680	–	−0.28 ± 0.13	0.01 ± 0.20	4559 ± 229	4.76 ± 0.59	0.48 ± 0.05	−0.18 ± 0.17
HD 53705	−0.16 ± 0.03	−0.04 ± 0.04	−0.04 ± 0.02	5825 ± 20	4.37 ± 0.10	1.20 ± 0.04	−0.19 ± 0.03
HD 53706	−0.26 ± 0.05	−0.07 ± 0.02	−0.01 ± 0.02	5260 ± 31	4.35 ± 0.11	0.74 ± 0.05	−0.26 ± 0.04
HD 57095	−0.15 ± 0.10	−0.04 ± 0.04	0.16 ± 0.08	4945 ± 54	4.45 ± 0.1	1.09 ± 0.08	−0.03 ± 0.06
HD 59686	0.29 ± 0.25	0.12 ± 0.06	0.36 ± 0.12	4871 ± 135	3.15 ± 0.24	1.85 ± 0.12	0.28 ± 0.18
HD 61606	−0.18 ± 0.10	0.00 ± 0.07	0.05 ± 0.06	4958 ± 80	4.45 ± 0.14	1.01 ± 0.12	0.01 ± 0.08
HD 64606	−0.51 ± 0.08	−0.39 ± 0.10	−0.36 ± 0.08	5351 ± 68	4.62 ± 0.07	0.92 ± 0.19	−0.71 ± 0.09
HD 65277	−0.26 ± 0.14	−0.08 ± 0.05	−0.05 ± 0.08	4843 ± 80	4.39 ± 0.16	0.99 ± 0.13	−0.26 ± 0.08
HD 65486	−0.44 ± 0.06	−0.24 ± 0.14	−0.25 ± 0.06	4660 ± 66	4.55 ± 0.13	0.82 ± 0.16	−0.33 ± 0.07
HD 65907	−0.19 ± 0.04	0.03 ± 0.04	0.00 ± 0.02	5979 ± 31	4.59 ± 0.12	1.36 ± 0.10	−0.29 ± 0.04
HD 67199	−0.13 ± 0.11	0.00 ± 0.14	0.20 ± 0.10	5136 ± 56	4.54 ± 0.08	0.84 ± 0.08	0.06 ± 0.06
HD 69830	−0.09 ± 0.05	0.08 ± 0.01	0.11 ± 0.02	5410 ± 26	4.38 ± 0.07	0.89 ± 0.03	−0.03 ± 0.04
HD 72673	−0.37 ± 0.05	−0.22 ± 0.06	−0.22 ± 0.03	5242 ± 28	4.50 ± 0.09	0.69 ± 0.05	−0.37 ± 0.04
HD 74576	−0.15 ± 0.06	0.04 ± 0.05	−0.03 ± 0.04	5000 ± 55	4.55 ± 0.13	1.07 ± 0.08	−0.03 ± 0.06
HD 76151	0.13 ± 0.03	0.20 ± 0.05	0.16 ± 0.03	5803 ± 29	4.50 ± 0.08	1.02 ± 0.04	0.14 ± 0.04
HD 82342	−0.27 ± 0.07	−0.14 ± 0.06	0.00 ± 0.08	4907 ± 78	4.46 ± 0.17	0.74 ± 0.15	−0.40 ± 0.08
HD 84117	0.05 ± 0.06	0.05 ± 0.05	0.03 ± 0.11	6167 ± 37	4.35 ± 0.10	1.42 ± 0.09	−0.03 ± 0.05
HD 85512	−0.31 ± 0.17	−0.06 ± 0.18	0.05 ± 0.17	4505 ± 176	4.71 ± 0.48	0.32 ± 1.15	−0.18 ± 0.19
HD 100623	−0.38 ± 0.09	−0.21 ± 0.07	−0.21 ± 0.07	5246 ± 37	4.54 ± 0.05	1.00 ± 0.06	−0.38 ± 0.05
HD 101581	−0.46 ± 0.09	−0.36 ± 0.08	−0.17 ± 0.08	4646 ± 96	4.8 ± 0.2	0.58 ± 0.35	−0.37 ± 0.09
HD 102365	−0.29 ± 0.08	−0.17 ± 0.04	−0.05 ± 0.03	5667 ± 27	4.59 ± 0.02	1.05 ± 0.06	−0.27 ± 0.04
HD 102438	−0.20 ± 0.04	−0.19 ± 0.02	−0.04 ± 0.04	5639 ± 51	4.6 ± 0.04	1.12 ± 0.1	−0.23 ± 0.06
HD 103166	0.39 ± 0.14	0.31 ± 0.02	0.70 ± 0.08	5325 ± 45	4.36 ± 0.07	0.95 ± 0.05	0.35 ± 0.05

Table 10. continued.

Star (HD)	[Na/H]	[Mg/H]	[Al/H]	$T_{\rm eff}$ [K]	$\log g$ [cm s^{-2}]	$\xi_{\rm t}$ [km s^{-1}]	[Fe/H]
HD 103932	0.21 ± 0.11	0.09 ± 0.08	0.40 ± 0.10	4874 ± 125	4.44 ± 0.26	1.3 ± 0.17	0.09 ± 0.13
HD 104304	0.35 ± 0.13	0.28 ± 0.08	0.42 ± 0.06	5562 ± 50	4.37 ± 0.06	1.1 ± 0.06	0.27 ± 0.06
HD 109200	−0.29 ± 0.05	−0.16 ± 0.06	−0.08 ± 0.06	5103 ± 46	4.47 ± 0.07	0.75 ± 0.07	−0.24 ± 0.05
HD 111261	−0.44 ± 0.07	−0.44 ± 0.12	−0.28 ± 0.09	4529 ± 62	4.44 ± 0.19	0.78 ± 0.17	−0.35 ± 0.08
HD 114386	−0.13 ± 0.10	0.09 ± 0.08	0.19 ± 0.07	4865 ± 93	4.3 ± 0.17	0.86 ± 0.12	−0.04 ± 0.07
HD 115617	0.00 ± 0.04	0.07 ± 0.08	0.18 ± 0.07	5577 ± 33	4.34 ± 0.03	1.07 ± 0.04	0.01 ± 0.05
HD 118972	−0.05 ± 0.10	0.11 ± 0.06	0.06 ± 0.08	5241 ± 66	4.43 ± 0.10	1.24 ± 0.08	−0.01 ± 0.08
HD 125072	0.29 ± 0.10	0.29 ± 0.04	0.57 ± 0.09	5001 ± 115	4.39 ± 0.21	1.21 ± 0.15	0.24 ± 0.11
HD 128620	0.37 ± 0.05	0.29 ± 0.09	0.43 ± 0.09	5844 ± 42	4.30 ± 0.04	1.18 ± 0.05	0.28 ± 0.06
HD 128621	0.23 ± 0.12	0.34 ± 0.12	0.44 ± 0.15	5199 ± 80	4.37 ± 0.12	1.05 ± 0.10	0.19 ± 0.09
HD 130922	−0.06 ± 0.17	−0.01 ± 0.07	−0.02 ± 0.07	4751 ± 73	4.32 ± 0.16	0.72 ± 0.13	−0.06 ± 0.07
HD 131977	−0.08 ± 0.12	0.01 ± 0.09	0.20 ± 0.07	4693 ± 80	4.36 ± 0.17	0.97 ± 0.16	0.07 ± 0.10
HD 135204	−0.07 ± 0.07	0.14 ± 0.12	0.18 ± 0.06	5332 ± 37	4.31 ± 0.04	0.84 ± 0.05	−0.11 ± 0.05
HD 136352	−0.23 ± 0.05	−0.03 ± 0.12	−0.03 ± 0.04	5667 ± 43	4.39 ± 0.03	1.08 ± 0.09	−0.31 ± 0.06
HD 140901	0.12 ± 0.06	0.19 ± 0.12	0.25 ± 0.07	5645 ± 37	4.4 ± 0.04	1.14 ± 0.05	0.13 ± 0.05
HD 142709	−0.77 ± 0.14	−0.24 ± 0.07	0.02 ± 0.10	4806 ± 106	4.6 ± 0.23	1.09 ± 0.19	−0.17 ± 0.11
HD 144628	−0.44 ± 0.11	−0.07 ± 0.10	−0.17 ± 0.06	5071 ± 43	4.41 ± 0.06	0.82 ± 0.07	−0.36 ± 0.05
HD 145417	−1.27 ± 0.09	−0.93 ± 0.11	−0.93 ± 0.07	5045 ± 111	4.74 ± 0.16	0.9 ± 0.43	−1.10 ± 0.15
HD 146233	0.03 ± 0.06	0.06 ± 0.05	0.13 ± 0.05	5786 ± 35	4.31 ± 0.03	1.18 ± 0.05	0.08 ± 0.05
HD 149661	−0.05 ± 0.08	0.07 ± 0.08	0.14 ± 0.05	5290 ± 52	4.39 ± 0.07	1.11 ± 0.07	0.04 ± 0.06
HD 150689	−0.20 ± 0.13	−0.06 ± 0.04	0.02 ± 0.09	4867 ± 87	4.43 ± 0.16	1.12 ± 0.13	−0.08 ± 0.07
HD 152391	−0.04 ± 0.09	–	0.06 ± 0.06	5521 ± 43	4.54 ± 0.05	1.29 ± 0.06	0.03 ± 0.05
HD 154088	0.30 ± 0.06	0.35 ± 0.05	0.47 ± 0.06	5414 ± 60	4.28 ± 0.08	1.14 ± 0.07	0.33 ± 0.07
HD 154363	−0.80 ± 0.15	−0.50 ± 0.07	−0.25 ± 0.14	4500 ± 161	4.78 ± 0.35	0.43 ± 0.05	−0.66 ± 0.26
HD 154577	−0.55 ± 0.06	−0.43 ± 0.10	−0.44 ± 0.06	4973 ± 55	4.73 ± 0.08	0.94 ± 0.12	−0.63 ± 0.06
HD 156026	−0.46 ± 0.09	−0.36 ± 0.15	−0.22 ± 0.10	4568 ± 94	4.67 ± 0.25	0.6 ± 0.26	−0.18 ± 0.09
HD 156274	−0.44 ± 0.09	−0.12 ± 0.08	−0.07 ± 0.07	5300 ± 32	4.41 ± 0.04	1.00 ± 0.05	−0.33 ± 0.04
HD 156384	−0.44 ± 0.15	−0.44 ± 0.07	−0.26 ± 0.11	4819 ± 110	4.66 ± 0.27	1.04 ± 0.22	−0.43 ± 0.12
HD 165185	−0.09 ± 0.06	−0.13 ± 0.05	0.11 ± 0.09	5942 ± 85	4.53 ± 0.05	1.39 ± 0.16	0.02 ± 0.10
HD 165499	−0.02 ± 0.05	−0.01 ± 0.06	0.11 ± 0.04	5950 ± 45	4.31 ± 0.02	1.14 ± 0.08	−0.01 ± 0.06
HD 170493	0.22 ± 0.11	0.20 ± 0.07	0.48 ± 0.09	4854 ± 120	4.49 ± 0.23	1.36 ± 0.2	0.15 ± 0.13
HD 170573	−0.06 ± 0.14	0.00 ± 0.05	0.16 ± 0.09	4767 ± 89	4.44 ± 0.2	1.07 ± 0.14	−0.07 ± 0.09
HD 170657	−0.23 ± 0.07	−0.16 ± 0.09	−0.08 ± 0.09	5115 ± 52	4.48 ± 0.08	1.13 ± 0.07	−0.22 ± 0.06
HD 172051	−0.28 ± 0.06	−0.23 ± 0.06	−0.05 ± 0.05	5634 ± 30	4.43 ± 0.03	1.06 ± 0.05	−0.20 ± 0.04
HD 177565	0.14 ± 0.05	0.09 ± 0.01	0.24 ± 0.06	5664 ± 28	4.43 ± 0.02	1.02 ± 0.04	0.14 ± 0.04
HD 189567	−0.24 ± 0.03	0.00 ± 0.04	−0.07 ± 0.01	5765 ± 24	4.43 ± 0.02	1.02 ± 0.04	0.14 ± 0.04
HD 191408A	−0.46 ± 0.09	−0.24 ± 0.04	−0.14 ± 0.04	5005 ± 45	4.38 ± 0.25	0.67 ± 0.09	−0.55 ± 0.06
HD 192310	0.00 ± 0.06	0.09 ± 0.04	0.13 ± 0.04	5069 ± 49	4.38 ± 0.19	0.79 ± 0.07	−0.01 ± 0.05
HD 196761	−0.3 ± 0.04	−0.13 ± 0.03	−0.13 ± 0.03	5435 ± 39	4.48 ± 0.08	0.91 ± 0.07	−0.29 ± 0.05
HD 207129	−0.03 ± 0.03	0.05 ± 0.03	0.01 ± 0.02	5910 ± 24	4.42 ± 0.05	1.14 ± 0.04	0.00 ± 0.04
HD 209100	–	−0.05 ± 0.04	−0.04 ± 0.06	4629 ± 77	4.36 ± 0.19	0.42 ± 0.25	−0.06 ± 0.08
HD 211415	−0.13 ± 0.04	−0.04 ± 0.02	−0.09 ± 0.04	5890 ± 30	4.51 ± 0.07	1.12 ± 0.07	−0.17 ± 0.04
HD 216803	–	0.01 ± 0.07	−0.09 ± 0.07	4555 ± 87	4.53 ± 0.26	0.66 ± 0.28	−0.01 ± 0.09
HD 222237	–	−0.07 ± 0.05	−0.07 ± 0.06	4747 ± 58	4.48 ± 0.22	0.40 ± 0.20	−0.31 ± 0.06
HD 222335	−0.22 ± 0.05	−0.06 ± 0.04	−0.11 ± 0.03	5260 ± 41	4.45 ± 0.11	0.92 ± 0.06	−0.16 ± 0.05